Reprogramming of cardiac phosphoproteome, proteome and transcriptome confers resilience to chronic adenylyl cyclase-driven stress

Jia-Hua Qu, Khalid Chakir, Kirill V. Tarasov, Daniel R. Riordon, Maria Grazia Perino, Allwin Jennifa Silvester, and Edward G. Lakatta *

Laboratory of Cardiovascular Science, Intramural Research Program, National Institute on Aging, National Institutes of Health, Baltimore, MD 21224, USA.

Address correspondence to:

Dr. Edward G. Lakatta*

Laboratory of Cardiovascular Science

Intramural Research Program

National Institute on Aging

National Institutes of Health

251 Bayview Boulevard

Suite 100

Baltimore, MD 21224

USA.

Tel: +1 410-558-8202

lakattae@grc.nia.nih.gov

Abstract

Our prior study discovered that numerous adaptive mechanisms emerge in response to cardiac-specific overexpression of adenylyl cyclase type 8 (TGAC8) which included overexpression of a large number of proteins. Here we conducted an unbiased phosphoproteomics analysis in order to determine the role of altered protein phosphorylation in the adaptive heart performance and protection profile of adult TGAC8 left ventricle (LV) at 3-4 months of age, and integrated the phosphoproteome with transcriptome and proteome. Based on differentially regulated phosphoproteins by genotype, numerous stress-response pathways within reprogrammed TGAC8 LV, including PKA, PI3K and AMPK signaling pathways, predicted upstream regulators (e.g., PDPK1, PAK1 and PTK2B), and downstream functions (e.g., cell viability, protein quality control), and metabolism were enriched. In addition to PKA, numerous other kinases and phosphatases were hyper-phosphorylated in TGAC8 vs. WT. Hyper-phosphorylated transcriptional factors in TGAC8 were associated with increased mRNA transcription, immune responses and metabolic pathways. Combination of the phosphoproteome with its proteome and with the previously published TGAC8 transcriptome enabled the elucidation of cardiac performance and adaptive protection profiles coordinately regulated at post-translational modification (PTM) (phosphorylation), translational and transcriptional levels. Many stress-response signaling pathways, i.e., PI3K/AKT, ERK/MAPK and ubiquitin labeling, were consistently enriched and activated in the TGAC8 LV at transcriptional, translational and PTM levels. Thus, reprogramming of the cardiac phosphoproteome, proteome and transcriptome confers resilience to chronic adenylyl cyclase-driven stress. We identified numerous pathways/function predictions via gene sets, phosphopeptides, and phosphoproteins, which may

point to potential novel therapeutic targets to enhance heart adaptivity, maintaining heart performance while avoiding cardiac dysfunction.

Keywords

left ventricle, adenylyl cyclase 8, AC-cAMP-PKA-Ca^{2+} signaling, phosphoproteome, proteome, transcriptome, PI3K/AKT signaling pathway

Introduction

Cardiac-specific overexpression of AC8 (TGAC8) markedly increases the heart rate and ejection fraction, similar to acute exercise but chronic and in the absence of corporal exertion, which persists on a 24 hours per day and 7 days per week basis[1-4]. Despite this constant high-level of heart performance driven by markedly elevated level of AC8-cAMP-PKA-Ca^{2+} signaling, which typically proceeds to near-term cardiac dysfunction, the TGAC8 survives for an extended period of time, up to about one year of age without excessive mortality[5]. Adaptive mechanisms that emerge in the TGAC8 heart confer resilience to this marked chronic stress of increased AC8-cAMP-PKA-Ca^{2+} signaling and include the enrichment and activation of a large number of proteins involved in multiple signaling pathways related to nutrient sensing, energy production, growth factor signaling, and cell proliferation[5].

As the body is a complex system, multiple levels of coordinated regulatory mechanisms are requisite to defend against stimuli and maintain health[6-9]. Phosphorylation is one of the most important and has been the most extensively studied post-translational modifications (PTM) of proteins. Various kinases and phosphatases within cells phosphorylate and dephosphorylate, respectively, a myriad of proteins to regulate their activities and affect multiple signaling

64 pathways. Because the PKA signaling pathway was highly enriched in TGAC8 vs. WT[5], we
65 reasoned that protein phosphorylation differed between TGAC8 and WT, and protein
66 phosphorylation modification plays a crucial role in the remarkable adaptative capacity of the
67 TGAC8 heart in response to markedly increased AC8-cAMP-PKA-Ca^{2+} signaling.

68 By the utilization of TMT-labeling mass spectrometry (MS), we identified 12963
69 phosphopeptides and 3646 phosphoproteins, and observed a general upregulation of
70 phosphorylation. By comparing genotypic differences in the proteome and phosphoproteome of
71 the present study with genotypic differences in the transcriptome published previously[5], we
72 sought to determine whether some adaptive mechanisms that emerge in the TGAC8 left ventricle
73 (LV) are regulated at transcriptional, translational and PTM (phosphorylation) levels. We
74 observed enrichments of phosphorylation, upregulation of kinase expression, and predicted
75 activation of upstream kinases to expand our understanding of the regulatory mechanisms the
76 TGAC8 utilizes to adapt to the chronic stress of activated AC8-cAMP-PKA-Ca^{2+} signaling. We
77 integrated genotypic difference between the TGAC8 and WT of the phosphoproteome with the
78 transcriptome and proteome, which broadened our understanding how changes in the
79 transcription, translation and PTM of proteins in the TGAC8 LV may singly or coordinately
80 enable the TGAC8 to endure the chronic AC8-induced stress.

81

82 **Materials and Methods**

83 **1. Animals**.

84 The cardiac-specific overexpression of AC8 (TGAC8) mouse, generated by inserting a cDNA
85 coding for human AC8 after the murine α-myosin heavy chain promoter, was a gift from Nicole

86 Defer/Jacques Hanoune, Unite de Recherches, INSERM U-99, Hôpital Henri Mondor, F-94010
87 Créteil, France. The three-month old male TGAC mice were used as study cases, and age
88 matched WT littermates, in the C57/BL6 background, were used as controls. All studies were
89 performed in accordance with the Guide for the Care and Use of Laboratory Animals published
90 by the National Institutes of Health (NIH Publication no. 85-23, revised 1996). The experimental
91 protocols were approved by the Animal Care and Use Committee of the National Institutes of
92 Health (protocol #441-LCS-2016).

93

94 **2. Isolate and store mouse heart.**

95 Three-month old male C57 mice (TGAC8 and WT) were euthanized, and the heart was isolated.
96 The left ventricle (LV) tissues were extracted and stored in tubes at -80°C.

97

98 **3. Mass spectrometry for phosphoproteome and data process.**

99 TGAC8 and WT LVs were sent to National Heart, Lung, and Blood Institute, National Institutes
100 of Health, Bethesda to conduct mass spectrometry (MS) using the standard tandem mass tag
101 (TMT) labeling method to obtain the phosphoproteome and total proteome concurrently in the
102 same platform. Mass spectrometry manipulation referred to our recently published paper[5].

103 Proteins from each group of samples are being quantified using the Bradford Assay Kit. Two-
104 hundred micrograms of protein from each group will be labeled with Amine-Reactive Tandem
105 Mass Tag Reagents (TMT Label Reagents; Thermo Scientific) according to the protocol supplied
106 by the manufacturer. Briefly, protein will be denatured followed by reduction (TCEP) and

107 alkylation (iodoacetamide) and then the alkylated proteins (200ug) for each sample were
108 precipitated in 6 volumes of ice-cold acetone at -20 °C overnight and later reconstituted in
109 Triethylammonium bicarbonate. Each sample was digested overnight using Trypsin enzyme
110 (enzyme to substrate ratio of 1:12.5) to get the peptide solution. Trypsin will cleave proteins at
111 lysine and arginine amino acid residues yielding tryptic peptides.

112 The 10-plex tandem mass tag (TMT) labeling was carried out according to Thermo Fisher
113 Scientific's TMT Mass Tagging kits protocol. Each of the TMT 10-plex label reagents were
114 reconstituted in Acetonitrile (ACN) and digested peptides from each sample were incubated with
115 specific tags (126, 127N, 127C, 128N, 128C, 129N, 129C, 130N,130C and 131 respectively) for
116 about 1 hour at room temperature. The TMT labeled samples are then combined and fractionated
117 using Off-Line high pH Basic Reverse Phase Fractionation to decrease the complexity of the
118 sample and to increase the number of peptides being identified into a total of 24 fractions which
119 will be later analyzed using LC-MS/MS. About 5% of the labeled tryptic peptides from each of
120 24-fractions were used for global proteomics analysis by nanoLC-MS/MS analysis while the
121 remaining 95% of samples in the 24-fractions were subjected to subsequent TiO2-enrichment for
122 quantitative phosphoproteomics analysis.

123 TiO2 enrichment was conducted using a Titansphere Phos-kit (GL biosciences Inc.). The TMT
124 10-plex tagged tryptic peptides were reconstituted in Buffer B (25% lactic acid in 1% TFA, 80%
125 Acetonitrile). The TiO2 SpinTip (1mg resin/10ul tip) was incubated with the sample, washed
126 using the wash buffer following manufacturers protocol and the phosphopeptides were eluted in
127 elution buffer sequentially using 5% ammonium hydroxide solution and 5% pyrrolidine solution.
128 The eluted fraction was dried and reconstituted in 0.1% FA for subsequent clean-up using the

129 ZipTip C18-tips (Millipore). The sample from elution fraction of C18-tips were dried and
130 reconstituted in 0.1%FA for LC-MS/MS analysis.

131 The flow-through fraction and the wash fraction from the TiO2 spinTip was collected, pooled
132 into a total of 6 fractions and speedvac dried which will be later used for Fe-IMAC
133 phosphoenrichment protocol. The peptide sample from 6-pooled flow-through fractions from
134 TiO2 enrichment underwent second round of phosphoenrichment using High-Select Fe-NTA
135 Phosphopeptide Enrichment Kit (Thermo Scientific). The eluted fraction was dried and
136 reconstituted in 0.1% FA for subsequent LC-MS/MS analysis.

137 Protein identification by LC-MS/MS analysis of peptides was performed using an Orbitrap
138 Fusion Lumos Tribid mass spectrometer (Thermo Fisher Scientific, San Jose, CA) interfaced
139 with an Ultimate 3000 Nano-HPLC apparatus (Thermo Fisher Scientific, San Jose, CA).
140 Peptides were fractionated by EASY-Spray PepMAP RPLC C18 column (2µm, 100A, 75 µm x
141 50cm) using a 120-min linear gradient of 5-35% ACN in 0.1% FA at a flow rate of 300 nl/min.
142 The instrument was operated in data-dependent acquisition mode (DDA) using FT mass analyzer
143 for one survey MS scan on selecting precursor ions followed by top 3 second data-dependent
144 HCD-MS/MS scans for precursor peptides with 2-7 charged ions above a threshold ion count of
145 10,000 with normalized collision energy of 37%. Survey scans of peptide precursors from 300 to
146 2000 m/z were performed at 120k resolution and MS/MS scans were acquired at 50,000
147 resolution with a mass range m/z 100-2000.

148 All MS and MS/MS raw spectra of TMT experiments from each set were processed and searched
149 using Sequest HT algorithm within the Proteome Discoverer 2.2 (PD2.2 software, Thermo Fisher
150 Scientific).The settings for precursor mass tolerance was set at 12 ppm, fragment ion mass
151 tolerance to 0.05 Da, trypsin enzyme with 2 mis cleavages with carbamidomethylation of

152 cysteine, TMT6-plex (lysine), TMT6-plex (peptide N-term) as fixed modification and
153 deamidation of glutamine and asparagine, oxidation of methionine as variable modifications.
154 The mouse sequence database from Swiss sprot was used for database search. Identified peptides
155 were filtered for maximum 1% FDR using the Percolator algorithm in PD 2.2 along with
156 additional peptide confidence set to high. Only peptide spectra containing all reporter ions were
157 designated as "quantifiable spectra" and used for peptide/protein quantitation. The final lists of
158 protein identification/quantitation were grouped and further filtered by PD 2.2 with at least 2
159 unique peptides per protein identified with high confidence. The quantitative protein ratios were
160 weighted and normalized by the median ratio for all quantifiable spectra of the peptides
161 pertaining to total protein identified.

162 For quantitative phosphopeptides analysis, an additional phosphorylation on Ser, Thr, Tyr
163 residues were specified as variable modifications. To confidently localize phosphorylation sites,
164 the phosphoRS 3.0 node integrated in PD 2.2 workflow was used. The algorithm of phosphoRS
165 3.0 software enables automated and confident localization of phosphosites by determining
166 individual probability values for each putatively phosphorylated site within the validated peptide
167 sequences. For each relative ratio group of phosphopeptides/sites, no normalization was applied.

168 To remove low quality signal, we remained peptides tagged with the medium and high
169 confidence. We divided the expressions of phosphoproteins to those of total proteins to obtain
170 the normalized phosphoproteome. As the expressions appeared to be near normal distribution,
171 we calculated the fold change by dividing the average value of TGAC8 samples by the average
172 value of WT samples, and calculated p-value using two-sided unpaired Student's t-test. Data
173 were deposited in MassIVE (ID: MSV000089850).

174

175 **4. Analyses of the TGAC8 LV transcriptome.**

176 The processed transcriptomic data were obtained from our recently published work (GEO:
177 GSE205234)[5]. The significantly changed mRNAs (TGAC8 vs. WT, q-value < 0.05) were
178 uploaded into DAVID[2] (version: 6.8; https://david.ncifcrf.gov/home.jsp) for Gene Ontology
179 (GO) term enrichments, and were also imported into Ingenuity Pathway Analysis[3] (IPA
180 (QIAGEN, March 2020)) for upstream kinases and phosphatases prediction. Kinases and
181 phosphatases were selected from the transcriptome and their changes at mRNA level were
182 displayed to observe their regulation by the overexpression of AC8.

183

184 **5. Analyses of phosphoproteome and proteome.**

185 Both unnormalized and normalized phosphoproteome were analyzed and visualized in PCA,
186 heatmap, and volcano plots. With the cutoff -log(p-value) > 1.3 and absolute(log2(fold change))
187 ≥ 0.4, we obtained the significantly changed unnormalized and normalized phosphoproteins
188 (TGAC8 vs. WT) and imported them into IPA for functional analyses respectively, and
189 compared the canonical pathway enrichments from these two datasets. In IPA, the upstream
190 kinases were predicted based upon the unnormalized phosphoproteom, and the regulatory
191 pathways from the predicted upstream kinases to downstream effective signaling pathways were
192 generated. Molecular and cellular functions were also enriched in IPA. The similar analyses to
193 those conducted in the TGAC8 LV transcriptome were also done in the TGAC8 LV total
194 proteome to observe the GO term enrichment, predicted activities of upstream kinases and
195 phosphatases, and expression of kinases and phosphatases at protein level.

196

197 **6. Analyses of phosphopeptides.**

198 The upregulated phosphopeptides (TGAC8 vs. WT, p-value < 0.05 and log2(fold change) > 0)
199 were processed in R. After split of peptides with multiple phosphosites into individual peptides
200 and filtering of ambiguously identified sites, 2264 phosphopeptides were selected. Protein
201 peptide sequences of full length were downloaded from Uniprot database[10] and matched to the
202 protein accessions corresponding to processed and selected phosphopeptides. Peptides centered
203 on the phosphosites and flanked by 6 amino acids on the N and C termini respectively were
204 extracted from the matched protein peptide sequences, and uploaded into WebLogo[11]
205 (http://weblogo.threeplusone.com/) and iceLogo[12] (https://iomics.ugent.be/icelogoserver/) for
206 sequence motif analysis. In WebLogo online analysis, different amino acids were labeled in
207 different colors representing different chemical properties (refer to figure legend). In iceLogo
208 online analysis, a public amphiphilicity index of polar amino acids reported by Mitaku and
209 colleagues[13] was used as an aid to characterize the amino acid preference at membrane-water
210 interfaces. In addition, the phosphopeptides of PI3K/AKT substates were summarized and
211 displayed in stacked bar plot.

212

213 **7. Integrative analyses of transcriptome, proteome and phosphoproteome.**

214 The changes of significantly regulated molecules (TGAC8 vs. WT, q-value or p-value < 0.05) in
215 transcriptome, total proteome, and unnormalized phosphoproteome were displayed in circos plot.
216 In addition, the changes at different level were compared and visualized in correlation scatter
217 plots. The discordant proteins whose change directions in total proteome and phosphoproteome

218 were opposite were used to analyze the specific regulation at the phosphorylation level by the
219 use of Reactome and GO (Cellular Component and Biological Process) databases.

220 As to the coordinated regulation, the above mentioned significantly regulated molecules
221 (TGAC8 vs. WT) in each dataset were imported into IPA for canonical pathway enrichment.
222 PI3K/AKT, ERK/MAPK and protein ubiquitination signaling pathways were coordinated across
223 all omics. The phosphopeptides of protein substrates of PI3K were extracted from the
224 phosphopeptide dataset and the numbers of changed phosphopeptides (TGAC8 vs. WT) were
225 summarized and visualized in stacked bar plot. The PI3K/AKT signaling pathway were
226 visualized in IPA, and nodes in the pathways were marked in different colors in terms of their
227 changes at different levels.

228 As kinases and phosphatases are pivotal in phosphorylation, and transcription factors (TFs) are
229 important in transcription regulation, they were extracted from transcriptome, proteome, and
230 phosphoproteome to observe their changes (TGAC8 vs. WT) and deduce their role in the
231 reprogram of phosphoproteome. The upstream transcription regulators including but not only
232 TFs were predicted on the basis of transcriptome and proteome by the utilization of knowledge
233 base in IPA, and their expressions were searched in multiple datasets. Furtherly, TFs that were
234 significantly regulated at phosphorylation level (TGAC8 vs. WT, $p\text{-value} < 0.05$) were defined
235 as significantly changed phosphorylated TFs in this research, and they were uploaded into
236 STRING database[4] (version: 11.0; http://string-db.org/) to generate protein-protein interaction
237 network and enrich KEGG pathways. They were also imported into IPA for canonical pathway,
238 molecular and cellular functions enrichments.

239

240 **8. Western blot.**

241 Snap-frozen left ventricle (LV) tissue from three-month-old male mice was homogenized and
242 lysed in ice cold RIPA buffer (Thermo Fisher Scientific: 25 mM Tris-HCl (pH 7.6), 150 mM
243 NaCl, 1% NP-40, 1% sodium deoxycholate, 0.1% SDS) supplemented with a Halt protease
244 inhibitor cocktail (Thermo Fisher Scientific), Halt phosphatase inhibitor cocktail (Thermo Fisher
245 Scientific) and 1 mM phenylmethyl sulfonyl fluoride, using a Precellys homogenizer (Bertin
246 Instruments) with tissue homogenization kit CKMix (Bertin Instruments) at 4 °C. Extracts were
247 then centrifuged at 10,000×g for 10 min at 4 °C and the protein concentration of the soluble
248 fraction determined using the Bicinchoninic Acid (BCA) Assay (Thermo Fisher Scientific).
249 Samples were denatured in Laemmli sample buffer (BioRad Laboratories) containing 355 mM 2-
250 mercaptoethanol at 95 °C for 5 min, and proteins (10–50 μg/lane) resolved on 4–20% Criterion
251 TGX Stain Free gels (Bio-Rad Laboratories) by SDS/PAGE. Gels then exposed to UV
252 transillumination for 2.5 min to induce crosslinking of Stain Free gel trihalo compound with
253 protein tryptophan residues. Proteins were then transferred to low fluorescence polyvinylidene
254 difluoride (LF-PVDF) membranes (BioRad Laboratories) using an electrophoretic transfer cell
255 (Mini Trans-Blot, Bio-Rad). Membrane total protein was visualized using an Amersham Imager
256 600 (AI600) (GE Healthcare Life Sciences) with UV transillumination to induce and a capture
257 fluorescence signal.

258 Blocked membranes (5% milk/tris-buffered saline with Tween-20, TBST) were incubated with
259 the following primary antibodies: (1) Anti-Phospho-PKA Substrate (RRXS*/T*) antibody, Cell
260 Signaling Technologies, Cat.#9624, 1:1000 dilution; (2) Anti-Ubiquitin antibody produced in
261 rabbit, Sigma-Aldrich, SAB1306582, 1:200 dilution; (3) Anti-pan-AKT antibody, Cell Signaling
262 Technologies, Cat.#4691, 1:1000 dilution; (4) Anti-Phospho-pan-AKT (Thr308) antibody, Cell

263 Signaling Technologies, Cat.#13038, 1:1000 dilution; (5) Anti-Phospho-pan-AKT (Ser473)
264 antibody, Cell Signaling Technologies, Cat.#4060, 1:1000 dilution; (6) Anti-AKT2 antibody,
265 Abcam, Cat.#13038, 1:1000 dilution; (7) Anti-Phospho-AKT2 (Ser473) antibody, Cell Signaling
266 Technologies, Cat.#ab131168, 1:1000 dilution; (8) Anti-ERK1/2 antibody, Cell Signaling
267 Technologies, Cat.#4695, 1:1000 dilution; (9) Anti-Phospho-ERK1/2 (Thr202/Tyr204) antibody,
268 Cell Signaling Technologies, Cat.#4376, 1:1000 dilution; (10) Anti-p21 Ras antibody, Cell
269 Signaling Technologies, Cat.#3965, 1:1000 dilution; (11) Anti-GAPDH antibody, Santa Cruz
270 Biotechnology, Cat.# sc-32233, 1:1000 dilution; (12) Anti-c-Raf antibody, ThermoFisher
271 Scientific, Cat.# PA5-29333, 1:1000 dilution; (13) Anti-Phospho-c-Raf (Ser338) antibody, Cell
272 Signaling Technology, Cat.# 9427, 1:1000 dilution; (14) Anti-MEK1/2 antibody, Cell Signaling
273 Technology, Cat.# 9126, 1:1000 dilution; (15) Anti-Phospho-MEK1/2 (Ser221) antibody, Cell
274 Signaling Technology, Cat.# 2338, 1:1000 dilution.

275 Primary antibodies were then detected using horseradish peroxidase (HRP) conjugated antibody
276 (Invitrogen) at 1:10,000. Bands were visualized using Pierce SuperSignal West Pico Plus ECL
277 substrate kits (Thermo Scientific), the signal captured using an Amersham Imager 600 (AI600)
278 (GE Healthcare Life Sciences) and quantified using ImageQuant TL software (GE Healthcare
279 Life Sciences). Band density was normalized to total protein. Two-tailed unpaired Student's t
280 test with Welch's correction was used for statistics.

281

282 **9. Protein synthesis detection.**

283 Protein synthesis was assessed by SUnSET-Western Blot as previously described in the above
284 section. Briefly, the puromycin solution was prepared in PBS, sterilized by filtration, and a

285 volume of 200 µl was injected in mice intraperitoneally, to achieve a final concentration of 0.04
286 µmol/g of body mass. After 30 min, mice were sacrificed, the LV was harvested and snap frozen
287 in liquid nitrogen. Protein extraction was performed using Precellys, quantified with BCA assay
288 25 µg of total protein were separated by SDS-PAGE; proteins were then transferred onto PVDF
289 membrane and incubated overnight in the anti-puromycin primary antibody (MABE343, Sigma-
290 Aldrich, St. Louis, MO). Visualization of puromycin-labeled bands were obtained using
291 horseradish peroxidase conjugated anti-mouse IgG Fc secondary antibody (Jackson
292 ImmunoResearch Laboratories Inc, West Grove, PA, USA), using Pierce Super Signal ECL
293 substrate kit (Pierce/ Thermo Scientific Rockford, IL). Chemiluminescence was captured with
294 the Imager AI600 and densitometry analysis was performed using ImageQuantTL software (both
295 by GE, Boston, MA). Total protein was used as control for protein loading. Genotypic
296 differences of protein synthesis were tested via an as unpaired t-test.

297

298 **10. Proteasome activity detection.**

299 Flash frozen tissue was homogenized in ice-cold cytosolic extraction buffer (50 mM Tris-HCl
300 pH 7.5, 250 mM Sucrose, 5 mM MgCl2, 0.5 mM EDTA, and 1 mM DTT). A bicinchoninic acid
301 (BCA) assay (Pierce) was used to determine the protein concentrations. All samples were equally
302 concentrated in proteasome assay buffer (50 mM Tris-HCl pH 7.5, 40 mM KCl, 5 mM MgCl2,
303 and 1 mM DTT). Proteasome activity was determined in the presence of 28 µM ATP using the
304 Suc-LLVY-AMC (18 µM, Boston Biochem #S280) fluorogenic substrate with and without
305 proteasome inhibition (MG 132, 1 mM, Sigma). The plate was read at an excitation wavelength
306 of 380 nm and an emission wavelength of 469 nm using a Spectramax M5 (Molecular Devices).

307 Activity was calculated by subtracting the background (proteasome inhibited value) from the
308 reading (proteasome activated value).

309

310 **11. Protein soluble and insoluble fractions detection.**

311 Protein aggregates were measured using Proteostat (Enzo, ENZ-51023) following the
312 manufacturer's instructions. For this assay left ventricle myocardial lysate (Cell Signaling lysis
313 buffer) was obtained, protein concentration assayed (BCA assay [Pierce]). Ten µg of protein
314 loaded into a 96-well microplate and protein aggregates were analyzed using the Proteostat assay
315 kit (Enzo Life Sciences) following the manufacturer's instructions. Background readings were
316 subtracted from sample recordings and were normalized to wild-type values.

317

318 **12. Data process and graphics production.**

319 Most raw data were precleared and processed using RStudio (version: 1.1.463) in R language
320 (version: 3.5.3), in which the tidyr package and dplyr package were applied. In addition,
321 GraphPad Prism (version: 7), Microsoft Excel (version: 2019) and Adobe Illustrator (version:
322 CC 2019) were also used for statistics and graphics. Venn diagrams were generated in Venny[5]
323 (version: 2.1.0; http://bioinfogp.cnb.csic.es/tools/venny/index.html). Circos plot was generated
324 using Circos software[6] in Perl language.

325

326 **Results**

327 **1. The TGAC8 reprograms the LV phosphoproteome.**

328 The TMT-labeling quantitative mass spectrometry (MS) identified **12963 phospho-peptides**
329 (File 1: Sheet 1) and **3646 phosphoproteins** (File 1: Sheet 2). The principal component analysis
330 (PCA) (Figure 1A) of the 3646 phosphoproteins in each mouse showed that the TG and WT
331 samples were distinguished into two groups completely. The heatmap (Figure 1B) showed the
332 intra-group consistency of upregulated phosphoproteins in TGAC8 compared to WT. Within the
333 cutoff at -log10(p-value) > 1.3 and absolute value of log2(fold-change(TG/WT)) ≥ 0.04, 781
334 phosphoproteins were differentially regulated by genotype. Of the 781 phosphoproteins, the
335 phosphorylation levels of 741 proteins were increased and only 40 were decreased in TGAC8 vs.
336 WT LV (Figure 1C).

337

338 **2. Functional analyses of the phosphoproteome.**

339 We performed the canonical pathway, upstream regulation, and downstream function analyses of
340 the remodeled LV phosphoproteome of TGAC8 using the Ingenuity Pathway Analysis (IPA)
341 software.

342 **2.1. Canonical pathway analysis of the remodeled LV phosphoproteome of TGAC8.**

343 To study the mechanisms at phosphorylation level, we first performed canonical pathway
344 analysis using IPA. Top canonical pathways within the phosphoproteome that were statistically
345 differentially enriched in TGAC8 vs. WT were displayed in the bar plot (Figure 1D and File 2:
346 Sheet 1). Of these pathways, cardiac hypertrophy signaling (enhanced) is most highly activated
347 (z-score as high as 4.867) (Figure 1D). The combination of Figure 1—figure supplement 1 and
348 File 2: Sheet 2 and our recently published work[5] showed that the phosphorylation status of
349 numerous molecules, e.g., Ca^{2+} ATPase, RyR2, Ncx, involved in excitation, calcium cycling,

350 contraction, relaxation and protein synthesis, was elevated in the TGAC8 vs. WT LV. However,
351 we have demonstrated that at three-month of age, the mouse age in the present study, the LV
352 mass is not elevated in TGAC8 vs. WT[5]. Of note, transcriptomic, proteomic and WB analyses
353 indicated that pathologic hypertrophic markers were not increased in TGAC8 vs. WT[5]. In this
354 regard, the activation of key stress response signaling pathways, e.g., protein kinase A (PKA)
355 signaling, PI3K signaling, and AMPK signaling, may protect against pathological changes, that
356 result in an increase in cardiac mass in TGAC8 despite its chronic increase in performance. For
357 example, activated PKA signaling can restrict the activity of AC8, acting as a feedback to fine-
358 tune the downstream signaling networks inside the body[14]. Additionally, nitric oxide (NO)
359 signaling may coordinate cardiac protection in the increase in cardiac mass (Figure 1D).
360 Increased phosphorylation status of HSP90 and Akt in TGAC8 synergistically increase eNOS
361 activity[15], and increased NO produced by eNOS may modulate the function of the ryanodine
362 receptor Ca^{2+} release channel (RyR2) on the cardiac sarcoplasmic reticulum[16]. The TMT-
363 labeling MS identified significant upregulated phosphorylation in the peptides of RyR2
364 (RISQTSQVSIDAAHGYSPR, E9Q401 [2805-2823]) (File 1: Sheet 1) , consistent with the PKA
365 induced phosphorylation of RyR2-S2809 mediating the increase in Ca^{2+} spark amplitude[17].

366 **2.2. Upstream regulators of the remodeled LV phosphoproteome of TGAC8.**

367 As known, the overexpression of AC8 activates the AC8-cAMP-PKA phosphorylation axis[4].
368 There were 2264 phosphosites whose names and locations are unambiguous within the 4990
369 upregulated phosphopeptides (p-value ≤ 0.05 and log2(fold-change(TG/WT)) ≥ 0) in TGAC8 vs.
370 WT. The majority of these phosphosites were serines (S) and threonines (T), and a few were
371 tyrosines (Y) (Figure 2A). By using WebLogo, we profiled the phosphorylation motif sequences
372 (Figure 2B). A typical PKA and AKT substate motif, R-R-X-pS/T, was the most abundant

373 substrate motif, consistent with increased PKA dependent phosphorylation (Figure 2B-2D)[18,19].
374 In addition to S and T, the center phosphosites also included phosphotyrosine (Y). The center
375 phosphosites were mainly flanked by the P-E-E sequence on the C terminus, endowing a strong
376 hydrophobic and acidic property to the C terminus of the substrate sequences (Figure 2B),
377 supported by the amphiphilicity index analysis in iceLogo (Figure 2D). Because phosphorylation
378 substrate motifs were not restricted to PKA's substrate motif, additional kinases must be also
379 involved in reprogramming the TGAC8 phosphoproteome. Therefore, we were inspired to
380 explore additional kinase-substrate pathways mediating the effect of the cardiac-overexpression
381 of AC8 here.

382 IPA predicted that 26 kinases were responsible for the above-mentioned phosphorylation motifs
383 (File 2: Sheet 3), among which, three had previously been identified to differ by genotype in the
384 LV transcriptome, 18 were shown to differ by genotype in the LV proteome, and 18 were
385 identified in the present phosphoproteome. Of note, most of the identified kinases were
386 upregulated in TGAC8 vs. WT at transcription, translation and PTM (phosphorylation) levels.
387 Within the phosphoproteome, eight kinases were predicted to be differentially activated by
388 genotype, and the phosphorylation level of four of these (PDPK1, PAK1, PTK2B and GSK3B)
389 was increased in TGAC8 vs. WT. These four kinases each phosphorylates various proteins to
390 regulate cellular functions. For example, a previous study observed that in human glioblastoma
391 cell lines, T98G and U87MG cells, the interference of human PDPK1 mRNA by siRNA
392 decreased the phosphorylation level of human BAD protein (S112, S136 and S155) and activated
393 cell death to suppress tumorigenesis[20]. Another study reported that in mouse myoblast cell line,
394 C2C12 cells, PDPK1 protein phosphorylated the mouse ULK1 protein[21]. Increased

395 phosphorylation states of BAD (upregulated at S112, S136 and S155) and ULK1 (upregulated at
396 S450, S521 and S637/638) in TGAC8 may be linked to activated PDPK1.

397 Different kinases can coordinate to reprogram the complex regulation network in the organism.
398 Consistent with the IPA canonical pathway analysis, the phosphorylation level of 27 proteins
399 (including the three kinases (PDPK1, PAK1 and PTK2B) auto-phosphorylating themselves)
400 were elevated by the three kinases to regulate cardiac stress signaling pathways, including PKA
401 signaling, ERK/MAPK signaling, cardiac hypertrophy signaling (enhanced), and renin-
402 angiotensin signaling (Figure 1E and Figure 1—figure supplement 2), to cope with the cardiac
403 stress in the TGAC8. For example, GSK3B is involved in multiple biological processes. PDPK1
404 phosphorylated GSK3B at S9[22,23] and PTK2B phosphorylated GSK3B at S9 and Y216[24,25] to
405 inhibit the kinase activity of GSK3B. In this phosphoproteome, GSK3B was phosphorylated at
406 multiple sites, including S9, Y216, S219 and S545, and thus GSK3B inhibition was linked to the
407 cardiac adaptation[26,27].

408 **2.3. Downstream functions of the remodeled LV phosphoproteome of TGAC8.**

409 To study the downstream functions of these phosphoproteins, we performed molecular and
410 cellular functions analysis in IPA. The enriched functions were mainly in three categories, i.e.,
411 cell viability, protein quality control, and metabolism (Figure 1F and File 2: Sheet5). The
412 functions of cellular assembly and organization, cellular function and maintenance, and cell
413 death and survival were ranked as the top three terms, indicating the important role of the
414 reprogrammed phosphoproteome in improving cell viability in response to the chronic stress of
415 the overexpression of AC8 in the mouse heart.

416

417 **3. Integrative analyses of transcriptome, proteome and phosphoproteome.**

418 We next integrated changes in PTM (phosphorylation) in TGAC8 vs. WT with genotypic
419 differences in protein translation and in transcription. The circos plot (Figure 3A) illustrates the
420 genotypic differences (TGAC8 vs. WT) in **molecules** identified across the transcriptome,
421 proteome, and phosphoproteome. In addition, the correlation scatter plots (Figure 3B)
422 demonstrated a moderate level of correlation of genotypic differences of molecular changes
423 within phosphoproteome and transcriptome, and a somewhat stronger correlation between
424 genotypic differences of molecular changes within phosphoproteome and proteome (Figure 3C).
425 Concordant and discordant enrichments of canonical pathways differed by genotype among the
426 three omics are shown in Figure 3D. A comparison of genotypic differences within the three
427 omics highlights the importance of protein phosphorylation, and the phosphorylation was
428 **coordinated with and supplemental to** transcription and translation.

429 Because kinases and phosphatases are the key regulators of phosphorylation, and
430 phosphorylation of transcription factors (TFs) are the primary determinant of their activities in
431 transcription, we compared genotypic differences in kinases, phosphatases and TFs within the
432 phosphoproteome and proteome with our previously published genotypic differences in the
433 TGAC8 vs. WT transcriptome[5] (Figure 3E). We identified 196 kinases, 71 phosphatases and 191
434 TFs in the present phosphoproteome (Figure 3F). The protein phosphorylation status of about
435 one half of these molecules differed significantly (p-value < 0.05) by genotype (Figure 3G), and
436 the protein phosphorylation status of majority of these molecules was increased (Figure 3H-3J).
437 The genotypic differences in the transcription (mRNA expression obtained from RNA-seq) and
438 translation (protein expression obtained from mass spectrometry) of these molecules, however,
439 differed from those in the phosphoproteome (Figure 3E). Because there were more molecules

440 that were unchanged or reduced in the TGAC8 vs. WT transcriptome or proteome than in the
441 phosphoproteome, it is clear that the changes in protein phosphorylation are of utmost
442 importance in the coordination of transcription, translation and PTM, that underlie the adaptive
443 response of the TGAC8 LV to the marked, chronic increase stress of its intrinsically activated
444 AC-cAMP-PKA-Ca^{2+} signaling. Thus, by utilizing multiple bioinformatic analysis methods, we
445 not only dissected the reprogrammed phosphoproteome and deduced its functions in the TGAC8
446 mouse LV, but also profiled the coordination of phosphoproteome, transcriptome and proteome.

447 **3.1. Implications of coordinated changes in protein phosphorylation and transcription in**
448 **TGAC8 vs. WT.**

449 The most likely type of coordination between protein phosphorylation and transcription is related
450 to phosphorylation states of TFs which is determined by kinases and phosphatases activities.
451 Analysis of the remodeled LV transcriptome of TGAC8 in Gene Ontology (GO) analysis using
452 DAVID online software discovered that enrichments of numerous phosphorylation and
453 dephosphorylation related biological processes and molecular functions significantly differed by
454 genotype (Figure 4A), and that the coordinated expression of numerous kinases and
455 phosphatases also differed by genotype (Figure 4B-4C and File 8). Because expression levels of
456 kinases and phosphatases do not denote their activation states, we utilized IPA to predict the
457 genotypic differences in activation states of upstream kinase and phosphatase (regulators of the
458 transcriptome). Intriguingly, 60 kinases were predicted to be upstream regulators of the
459 remodeled LV transcriptome of TGAC8, and the majority of these kinases were predicted to be
460 activated in TGAC8 vs. WT (Figure 4D and File 9). In contrast, much fewer phosphatases were
461 predicted between TGAC8 and WT, and most of these were predicted to be inhibited (Figure 4E
462 and File 9). Thus, the differential genotypic enrichment of phosphorylation status and predicted

463 activation of kinases and phosphatases identified in our post hoc analysis of our previously
464 reported TGAC8 vs. WT transcriptome[5] are linked to the differential genotypic reprogramming
465 of the phosphoproteome discovered in the present study.

466 We utilized IPA to predict the activation states of upstream transcription regulators on the basis
467 of the remodeled LV transcriptomes and proteomes, and then determined their expression levels
468 in transcriptome, proteome and phosphoproteome (Figure 4F). Because TFs are the main
469 regulators of transcription, and because phosphorylation of TFs usually regulates their
470 activities[28-30], we focused our subsequent analysis on functions of those TFs that were
471 differentially phosphorylated in TGAC8 vs. WT. To confirm the hypothesis that the TGAC8
472 might exert transcriptional control by TFs phosphorylation, we retrieved all TFs identified in our
473 previous transcriptome and proteome[5] and mapped them to the current phosphoproteome in order
474 to determine their genotypic differences in phosphorylation status. Of the 191 TFs also identified
475 in this phosphoproteome, 92 TFs differed significantly by genotype in phosphorylation status (p-
476 value < 0.05). In agreement with the general upregulated transcription in TGAC8 LV[5], nearly all
477 of the TFs that differed by genotype had increased phosphorylation level (Figure 4G and File 3).
478 The only exception was purine rich element binding protein G (Purg), known to be hyper-
479 phosphorylated in solid tumors[31].

480 We conducted Kyoto Encyclopedia of Genes and Genomes (KEGG) pathway analysis to further
481 probe the predicted facts of TFs that were generally hyper-phosphorylated in TGAC8 vs. WT.
482 Numerous immunity related pathways, cancer related pathways, and metabolism related
483 pathways were enriched (Figure 4H and File 4). We then utilized IPA for in-depth analysis.
484 Numerous metabolic canonical pathways (glucocorticoid receptor signaling and PPAR
485 signaling), a cancer related canonical pathway (regulation of epithelial-mesenchymal transition

486 pathway), and immunity related canonical pathways (role of JAK1, JAK2 and TYK2 in
487 interferon signaling, IL-9 signaling, JAK/Stat signaling, etc.) were enriched (Figure 4I and File
488 5: Sheet 1). Intriguingly, the sumoylation pathway was markedly inhibited. Because both
489 sumoylation and phosphorylation are important PTMs in transcriptional regulation[32,33], it is
490 possible that the upregulated protein phosphorylation and inhibited protein sumoylation pathway
491 in TFs coordinately activate transcription and improve immunity in the TGAC8 LV. In addition,
492 cell viability and metabolism in molecular and cellular functions were enriched in TGAC8 vs.
493 WT (Figure 4J and File 5: Sheet 2), consistent with enrichments of aforementioned KEGG
494 pathways and IPA canonical pathways (Figure 4H and 4I).

495 Taken together, we have discovered the existence of substantial crosstalk between protein
496 phosphorylation and transcription in the TGAC8 LV: phosphorylation of TFs reprograms
497 immunity and metabolism related pathways and functions in the TGAC8 LV, likely serving to
498 maintain cell survival in response to the chronic stress of marked AC8 overexpression.

499 **3.2. Coordinated changes in protein expression and phosphorylation of the remodeled**
500 **proteome and phosphoproteome of TGAC8.**

501 Having discovered the coordinated changes in the remodeled TGAC8 transcriptome and
502 phosphoproteome (Figure 4A-4E), we next sought to discover the extent to which changes in the
503 remodeled phosphoproteome of the TGAC8 LV were coordinated with changes in its remodeled
504 proteome. Numerous biological processes and molecular functions that were related to
505 phosphorylation and dephosphorylation were enriched in the remodeled TGAC8 LV proteome
506 (Figure 5A), as were numerous kinases and phosphatases (Figure 5B-5C and File 10). Twenty-
507 nine kinases that differed by genotype were predicted to be upstream regulators of the proteome,
508 and most of these were predicted to be activated in TGAC8 vs. WT. Fewer phosphatases than

509 kinases that differed by genotype were identified as upstream regulators of the remodeled
510 TGAC8 LV proteome (Figure 5D-5E and File 11).

511 One strategy adopted to probe deeper into the coordinated changes in the proteome and
512 phosphoproteome of the TGAC8 LV was to normalize the phosphoproteome to the total
513 proteome (in other words, to divide the phosphorylation expression by protein expression) (File
514 1: sheet4). Of the 3927 phosphoproteins identified in our mouse LV samples, 2164 were
515 identified in both the proteome and phosphoproteome, and these were focused for subsequent
516 analyses. After normalization, WT and TGAC8 samples manifested clear genotypic differences
517 in PCA analysis (Figure 5G), and phosphorylation status of numerous proteins normalized to the
518 protein expression level still differed by genotype without cutoff (Figure 5H) and with cutoff (-
519 log(p-value) > 1.3 and absolute(log2(TG/WT)) ≥ 0.4) (Figure 5I). Even after normalizing the
520 phosphorylation level to the protein expression level, the enrichments of canonical pathways in
521 TGAC8 were quite consistent with those of unnormalized phosphoproteome (Figure 5J and File
522 6). Cardiac hypertrophy signaling (enhanced) and cardiac hypertrophy signaling took the top two
523 places, emphasizing the important role of phosphorylation in the regulation of cardiac functions
524 in response to chronic stress when coordinated with changes in the total proteome.

525 Many important stress-response signaling pathways were enriched from phosphoproteome, e.g.,
526 PKA signaling, ERK/MAPK signaling, insulin receptor signaling, and PI3K/AKT signaling
527 (Figure 6A). Three of these pathways, PI3K/AKT, ERK/MAPK and ubiquitin labeling, were also
528 markedly enriched in our previous analysis on total proteome in TGAC8 LV[5]. By integrating and
529 comparing the enrichments from transcriptome, proteome and phosphoproteome, we were able
530 to identify the three signaling pathways in the TGAC8 LV, PI3K/AKT, ERK/MAPK and
531 ubiquitin labeling, that were regulated concordantly in transcription, translation, and PTM

532 (phosphorylation) (Figure 6B). WB validated activation of PI3K/AKT signaling pathway in
533 TGAC8, reproducing the results of our prior study using different antibodies (Figure 6C-6D and
534 Figure 6—figure supplement 1A (more significant)). We also demonstrated in that study that
535 ERK/MAPK signaling was also activated in TGAC8 vs. WT (Figure 6—figure supplement 1B-
536 C). Activation of PI3K/AKT and ERK/MAPK signaling is crucial for enhanced protein quality
537 control (the increase in protein synthesis and degradation) in the TGAC8 LV[5] (Figure 6—figure
538 supplement 1D- G). Although protein ubiquitination, an important process in protein
539 degradation, was enriched in TGAC8 LV within IPA analysis, its activity could not be predicted
540 on the basis of present knowledge base of IPA. Its WB analysis, however, indicated that
541 ubiquitination is indeed increased in TGAC8 vs. WT (Figure 6E).

542 We next sought to identify which molecules linked to PI3K/AKT signaling (one of the most
543 important pathways in this mouse model) differed in TGAC8 vs. WT. Among the significantly
544 changed upstream molecules, the majority were upregulated. AKT, a central molecule in the
545 pathway, was also increased in proteome and phosphoproteome (Figure 6F). By searching and
546 mapping the substrates of AKT, we unraveled that the phosphorylation levels of AKT peptide
547 substrates were mostly elevated in TGAC8 vs. WT (Figure 6G). Therefore, the downstream
548 effects and functions of AKT signaling were activated in TGAC8 LV: (1) upregulating GSK3 to
549 improve energy metabolism; (2) activating mTOR pathway to increase protein synthesis and cell
550 growth; (3) promoting NF-κB mediated transcription; (4) upregulating BAD and eNOS only at
551 phosphorylation level to enhance cell survival and cardiovascular functions. In summary, to
552 adapt the heart to stress for improved survival, the TGAC8 reprogram the cardiac LV
553 phosphoproteome to a large degree.

554

555 **4. Discordant regulation of the phosphoproteome and proteome in TGAC8 LV.**

556 Among the 443 proteins that differed by genotype in both protein phosphorylation and protein
557 expression levels, 33 were changed discordantly at the two levels (in opposite directions, i.e.,
558 upregulated in proteome but downregulated in phosphoproteome, or vice versa) (Figure 7A and
559 File 7: Sheet 1). We uploaded the 33 discordant proteins into STRING online software for
560 functional analyses. The GO_CC (Cellular Component) analysis resulted in many
561 **mitochondrial components**, indicating the involvement of phosphorylated proteins in
562 mitochondria (Figure 7B and File 7: Sheet 2). Reactome pathway analysis showed that in
563 addition to mitochondria, metabolic pathways were enriched significantly in TGAC8 (Figure 7C
564 and File 7: Sheet 3). Mitochondria are the hub of metabolism and multiple metabolic processes
565 are executed in mitochondria. Consistently, both metabolism and mitochondria related processes
566 were ranked the top processes in GO_BP (Biological Process) analysis (Figure 7D and File 7:
567 Sheet 4). Therefore, the discordant part between total proteome and phosphoproteome indicated
568 that the phosphorylation plays a critical role in the regulation of mitochondria and metabolism in
569 the TGAC8, distinct from its role in regulation at the translational level.

570

571 **5. Deduced schematic of coordination of phosphoproteome with transcriptome and**
572 **proteome in TGAC8 mouse LV.**

573 A deduced schematic integration of the remodeled phosphoproteome, proteome and
574 transcriptome of the TGAC8 LV is shown in Figure 8. The TGAC8 mouse initially induces a
575 PKA dependent phosphorylation via AC8-cAMP-PKA axis. Many cytoplasmic proteins
576 including TFs are thus phosphorylated and then transported into the nucleus where TFs

577 recognize and bind to the promoters to activate the transcription of more regulatory factors,
578 including kinases, phosphatases, and TFs. The activation states of these factors are changed upon
579 phosphorylated in cytosol, thereby activating additional kinases-controlled phosphorylation
580 cascades and reprogramming the cardiac phosphoproteome comprehensively.

581

582 **Discussion**

583 The major novel findings of the present study were differentially regulated phosphoproteins by
584 genotype and the enrichment of numerous stress-response pathways within the reprogrammed
585 TGAC8 LV, including PKA, PI3K and AMPK signaling pathways, their predicted upstream
586 regulators (e.g., PDPK1, PAK1 and PTK2B), and downstream functions (e.g., cell viability,
587 protein quality control, and metabolism). In addition to PKA, numerous other kinases and
588 phosphatases were hyper-phosphorylated in TGAC8 vs. WT. Hyper-phosphorylated
589 transcriptional factors in TGAC8 were associated with increased mRNA transcription, immune
590 responses and metabolic pathways. Integration of the phosphoproteome with its proteome and
591 with the previously published TGAC8 transcriptome enabled the elucidation of cardiac
592 performance and adaptive protection profiles that were coordinately regulated at PTM
593 (phosphorylation), translational and transcriptional levels. Many stress-response signaling
594 pathways, i.e., PI3K/AKT, ERK/MAPK and ubiquitin labeling, were consistently enriched and
595 activated in the TGAC8 LV at transcriptional, translational and PTM levels.

596 Most previous studies of PKA-dependent phosphorylation via the AC8-cAMP-PKA axis (typical
597 substrate motif of PKA dependent phosphorylation) focused on PKA phosphorylated targets as
598 downstream effects of activated AC8. For example, AC8 induced cAMP activates PKA to

599 increase the phosphorylation of many key proteins in cardiovascular system, e.g., ryanodine-
600 receptor-type 2 (RyR2), L-type Ca^{2+} channels (LTCC), phospholamban (PLN or PLB), etc[5]. Our
601 study identified 29 phosphosites on RyR2, 15 phosphosites on LTCC alpha 1 and beta 2, and 2
602 phosphosites (S16 and T17) on PLN, and, most interestingly, 7 phosphosites on SERCA2
603 (Sarcoplasmic/endoplasmic reticulum calcium ATPase 2), with the majority of these increased in
604 phosphorylation statuses in the TGAC8 LV (File 1: Sheet 1). It is worth noting that PLN is
605 phosphorylated on S16 by PKA whereas on T17 by Ca^{2+}-calmodulin-dependent protein kinase
606 (CaMKII)[34].

607 Following phosphorylation, many cytoplasmic proteins, including TFs, are transported into the
608 nucleus. TFs recognize and bind to the promoters to activate transcription, and many TFs were
609 hyper-phosphorylated in TGAC8 vs. WT (Figure 4 F and 4G). The phosphorylation of
610 STAT1[35,36], STAT3[36], HTT[37] and CREB1[38] is associated with the activation of their
611 transcriptional activities. Elevated TFs phosphorylation and possibly activated transcription were
612 consistent with the general increase in transcriptome in TGAC8[5]. The hyper-phosphorylated TFs
613 might contribute to the improved immunity, metabolism and cell viability in TGAC8 (Figure 4H
614 and 4I). For example, STAT family proteins are transcription activators, and their
615 phosphorylation is involved in inflammation and immune response[39,40]. The present study
616 identified increased phosphorylation levels in S727 on STAT1 and S726/S727 on STAT3 (File
617 1: Sheet 1), in line with our previous report which identified hyper-phosphorylation of
618 components within inflammation and immune response signaling pathways such as JAK/STAT
619 and JNK pathways[5].

620 Upon activation of RNA transcription, expression of numerous molecules, including TFs,
621 kinases, and phosphatases was increased in TGAC8 vs WT, thereby, leading to activation of

622 other kinase-controlled phosphorylation cascades in addition to PKA. For example, among the
623 others, IPA predicted activation of PDPK1, PAK1 and PTK2B directed signaling in TGAC8 vs
624 WT. In the context of the overexpression of AC8, these three kinases could be activated to
625 phosphorylate multiple proteins to activate the PKA pathway (positive feedback) and the
626 MAPK/ERK pathway (also known as Ras-Raf-MEK-ERK pathway) to maintain heart health
627 (Figure 1E and Figure 1—figure supplement 2). Previously, we showed WB results confirming
628 MAPK/ERK pathway activation due to increased protein expression of p21 Ras and the elevated
629 phosphorylation levels of c-Raf, MEK1/2 and ERK1/2 as well as their increased ratios of
630 phosphorylation to protein expression[5]. In the present study, S233 and S621/S641 on Isoform 2
631 of RAF proto-oncogene serine/threonine-protein kinase were hyper-phosphorylated in TGAC8
632 (File 1: Sheet 1). Importantly, the multifunctional molecule, GSK3B, was downstream of PDPK1
633 and PTK2B in the integrated regulation network. GSK3B is involved in metabolism and cardiac
634 hypertrophy[41,42]. Interestingly, AC8 is required for glucose homeostasis and hypothalamic
635 adaptation to high-fat diet[43]. The phosphorylation of GSK3B is also a critical mediator in
636 convergence of cardioprotection signaling[26,27]. We previously detected the increase in the protein
637 expression of GSK3B[5] and here identified the hyper-phosphorylated S9 on GSK3B (File 1: Sheet
638 1).

639 Taken together, the TGAC8 upregulates phosphorylation to reprogram the heart. Based on
640 results in this study, combined with our recently published work on TGAC8 LV[5], we generated a
641 comprehensive circuitry (Appendix 1). Navigating this figure "by the numbers": marked,
642 chronic, cardiac specific overexpression of AC8 (1) chronically increases cAMP (2) and PKA-
643 Ca^{2+} signaling (3), resulting, not only in an incessantly increased cardiac performance, due to
644 elevated heart rate and LV contractility (4), but also activation of growth factor signaling

645 pathways (5), leading to increase in energy demand due to increased transcription and increased
646 amino acid, nucleotide, protein, lipid and lipoprotein synthesis, increased protein quality control,
647 including proteosome activity, autophagy, mitophagy, cytokine signaling and inflammation (6).
648 Chronic high level of AC8 activation elicits numerous stress responses (8) including increased
649 nutrient sensing with increased AMPK signaling (10A), increased ROS scavenging, protection
650 against cell death, and also induction of signaling to minimize the impact of AC-PKA signaling
651 (10B). Shifts in energy production and utilization to deal with the marked energy demands of the
652 TGAC8 heart (10, 12) include: enhancement of glucose metabolism is pronounced (11, 13),
653 whilst utilization of fatty acids to produce energy is reduced (11) but an increase in glucose
654 catabolism (10, 11) is accompanied by an increased anabolism (12), supported by increased
655 aerobic glycolysis (11,13); increased utilization of the pentose phosphate shunt (5, 13) supports
656 increased amino acid, nucleotide, protein and lipoprotein synthesis induced by growth factor
657 signaling (5), resulting in an increase in LV biomass (14). This adaptive profile balances energy
658 requirements necessary for an incessant marked increase in cardiac performance (4), for
659 increased RNA transcription, protein translation and quality control required for cardiac growth
660 (14), and for other biological processes within the LV myocardium (6). This pattern of consilient
661 adaptations (6-15) sustains an incessant increase in cardiac performance while conferring cardio-
662 protection to the TGAC8 heart.

663 **Summary and Future Perspectives**

664 The reprogrammed phosphoproteome activated stress response signaling pathways to defend
665 against cardiac stress in young mice, improve cell viability and suppress cell death. On one hand,
666 the reprogramed phosphoproteome enhances transcription to improve the immunity and
667 metabolism; on the other hand, it coordinates with the proteome to improve mitochondrial

668 functions and metabolism. Finally, although we revealed the coordination of regulation at
669 different levels, which provides a roadmap to guide the integration of transcription, translation
670 and PTM, our results set the stage for additional studies in this remarkable TGAC8 model: What
671 kinases are specifically involved in the PTM identified here? How are these phosphorylated
672 proteins specifically distributed in subcellular locations? Also, the specific details of how
673 PDPK1, PAK1 and PTK2B directed signaling is activated by overexpression of AC8 requires
674 further study. The bioinformatic analysis strategy here revealed a larger kinase-substrate network
675 important in the remodeling of the TGAC8 heart. We plan to validate these kinase-substrate
676 reactions in additional follow-up studies and provide the reliable mechanism in cardiovascular
677 research.

678 The present study focuses on a comprehensive in silico analysis of functionally coherent and
679 data-driven transcription, translation, and post-translation patterns that were well translated in the
680 contribution to AC8-overexpression cardiac outcomes, while further investigation is warranted to
681 see whether the hub pathway/function predictions via gene sets, phosphopeptides, and
682 phosphoproteins could be used as biomarkers or impact the diagnostic specificity for transgenic
683 AC8 cardiac health and pathology, and even be used as therapeutic targets to enhance heart
684 adaptivity, maintaining heart performance while avoiding cardiac dysfunction.

685

686 **Acknowledgements**

687 We thank all members in Laboratory of Cardiovascular Science, National Institute on Aging,
688 National Institutes of Health, for technical assistance and discussion. This work utilized the
689 computational resources of the NIH HPC Biowulf cluster (http://hpc.nih.gov).

Funding

Intramural Research Program, National Institute on Aging, National Institutes of Health.

Disclosures

None.

References

1 Lipskaia, L. *et al.* Enhanced cardiac function in transgenic mice expressing a Ca(2+)-stimulated adenylyl cyclase. *Circ. Res.* **86**, 795-801 (2000). https://doi.org:10.1161/01.res.86.7.795

2 Georget, M. *et al.* Augmentation of cardiac contractility with no change in L-type Ca2+ current in transgenic mice with a cardiac-directed expression of the human adenylyl cyclase type 8 (AC8). *Faseb j* **16**, 1636-1638 (2002). https://doi.org:10.1096/fj.02-0292fje

3 Esposito, G. *et al.* Increased myocardial contractility and enhanced exercise function in transgenic mice overexpressing either adenylyl cyclase 5 or 8. *Basic Res Cardiol* **103**, 22-30 (2008). https://doi.org:10.1007/s00395-007-0688-6

4 Moen, J. M. *et al.* Overexpression of a Neuronal Type Adenylyl Cyclase (Type 8) in Sinoatrial Node Markedly Impacts Heart Rate and Rhythm. *Front Neurosci* **13**, 615 (2019). https://doi.org:10.3389/fnins.2019.00615

5 Tarasov, K. V. *et al.* A remarkable adaptive paradigm of heart performance and protection emerges in response to the constitutive challenge of marked cardiac-specific overexpression of adenylyl cyclase type 8. *eLife* **11**, e80949 (2022). https://doi.org:10.7554/eLife.80949

6 Qu, J.-H. *et al.* Proteomic Landscape and Deduced Functions of the Cardiac 14-3-3 Protein Interactome. *Cells* **11**, 3496 (2022). https://doi.org:10.3390/cells11213496

7 Zhang, R. *et al.* Caloric Restriction Induces MicroRNAs to Improve Mitochondrial Proteostasis. *iScience* **17**, 155-166 (2019). https://doi.org:https://doi.org/10.1016/j.isci.2019.06.028

8 Pei, J. F. *et al.* Diurnal oscillations of endogenous H(2)O(2) sustained by p66(Shc) regulate circadian clocks. *Nature cell biology* **21**, 1553-1564 (2019). https://doi.org:10.1038/s41556-019-0420-4

9 Deng, C., Qu, J.-H., Kim, I. & Tang, X. Histone crotonylation in neurobiology: to be or not to be? *Chin. Med. J.* **135**, 1036-1038 (2022). https://doi.org:10.1097/cm9.0000000000001945

10 Consortium, T. U. UniProt: a worldwide hub of protein knowledge. *Nucleic Acids Res.* **47**, D506-D515 (2018). https://doi.org:10.1093/nar/gky1049

11 Crooks, G. E., Hon, G., Chandonia, J. M. & Brenner, S. E. WebLogo: a sequence logo generator. *Genome research* **14**, 1188-1190 (2004). https://doi.org:10.1101/gr.849004

725 12 Colaert, N., Helsens, K., Martens, L., Vandekerckhove, J. & Gevaert, K. Improved visualization of
726 protein consensus sequences by iceLogo. *Nat Methods* **6**, 786-787 (2009).
727 https://doi.org:10.1038/nmeth1109-786
728 13 Mitaku, S., Hirokawa, T. & Tsuji, T. Amphiphilicity index of polar amino acids as an aid in the
729 characterization of amino acid preference at membrane-water interfaces. *Bioinformatics* **18**,
730 608-616 (2002). https://doi.org:10.1093/bioinformatics/18.4.608
731 14 Willoughby, D. *et al.* A key phosphorylation site in AC8 mediates regulation of Ca(2+)-dependent
732 cAMP dynamics by an AC8-AKAP79-PKA signalling complex. *J Cell Sci* **125**, 5850-5859 (2012).
733 https://doi.org:10.1242/jcs.111427
734 15 Takahashi, S. & Mendelsohn, M. E. Synergistic activation of endothelial nitric-oxide synthase
735 (eNOS) by HSP90 and Akt: calcium-independent eNOS activation involves formation of an
736 HSP90-Akt-CaM-bound eNOS complex. *The Journal of biological chemistry* **278**, 30821-30827
737 (2003). https://doi.org:10.1074/jbc.M304471200
738 16 Lim, G., Venetucci, L., Eisner, D. A. & Casadei, B. Does nitric oxide modulate cardiac ryanodine
739 receptor function? Implications for excitation-contraction coupling. *Cardiovasc Res* **77**, 256-264
740 (2008). https://doi.org:10.1093/cvr/cvm012
741 17 Meissner, G. in *Structure and Function of Calcium Release Channels Current Topics in*
742 *Membranes* 91-113 (2010).
743 18 Hunzicker-Dunn, M. E. *et al.* PKA and GAB2 play central roles in the FSH signaling pathway to
744 PI3K and AKT in ovarian granulosa cells. *Proceedings of the National Academy of Sciences of the*
745 *United States of America* **109**, E2979-2988 (2012). https://doi.org:10.1073/pnas.1205661109
746 19 Bellis, A. *et al.* Cross-talk between PKA and Akt protects endothelial cells from apoptosis in the
747 late ischemic preconditioning. *Arterioscler Thromb Vasc Biol* **29**, 1207-1212 (2009).
748 https://doi.org:10.1161/atvbaha.109.184135
749 20 Desai, S., Pillai, P., Win-Piazza, H. & Acevedo-Duncan, M. PKC-iota promotes glioblastoma cell
750 survival by phosphorylating and inhibiting BAD through a phosphatidylinositol 3-kinase pathway.
751 *Biochim Biophys Acta* **1813**, 1190-1197 (2011). https://doi.org:10.1016/j.bbamcr.2011.03.007
752 21 Li, Y. *et al.* microRNA-378 promotes autophagy and inhibits apoptosis in skeletal muscle.
753 *Proceedings of the National Academy of Sciences of the United States of America* **115**, E10849-
754 e10858 (2018). https://doi.org:10.1073/pnas.1803377115
755 22 Chen, X. *et al.* PDK1 regulates platelet activation and arterial thrombosis. *Blood* **121**, 3718-3726
756 (2013). https://doi.org:10.1182/blood-2012-10-461897
757 23 Ericson, K. *et al.* Genetic inactivation of AKT1, AKT2, and PDPK1 in human colorectal cancer cells
758 clarifies their roles in tumor growth regulation. *Proceedings of the National Academy of Sciences*
759 *of the United States of America* **107**, 2598-2603 (2010).
760 https://doi.org:10.1073/pnas.0914018107
761 24 Hartigan, J. A., Xiong, W. C. & Johnson, G. V. Glycogen synthase kinase 3beta is tyrosine
762 phosphorylated by PYK2. *Biochemical and biophysical research communications* **284**, 485-489
763 (2001). https://doi.org:10.1006/bbrc.2001.4986
764 25 Tsai, C. C. *et al.* Glycogen synthase kinase-3beta facilitates IFN-gamma-induced STAT1 activation
765 by regulating Src homology-2 domain-containing phosphatase 2. *J Immunol* **183**, 856-864 (2009).
766 https://doi.org:10.4049/jimmunol.0804033
767 26 Juhaszova, M. *et al.* Glycogen synthase kinase-3beta mediates convergence of protection
768 signaling to inhibit the mitochondrial permeability transition pore. *The Journal of clinical*
769 *investigation* **113**, 1535-1549 (2004). https://doi.org:10.1172/JCI19906
770 27 Juhaszova, M. *et al.* Role of glycogen synthase kinase-3beta in cardioprotection. *Circ. Res.* **104**,
771 1240-1252 (2009). https://doi.org:10.1161/CIRCRESAHA.109.197996

28 Bohmann, D. Transcription factor phosphorylation: a link between signal transduction and the regulation of gene expression. *Cancer cells (Cold Spring Harbor, N.Y. : 1989)* **2**, 337-344 (1990).
29 Weigel, N. L. & Moore, N. L. Steroid receptor phosphorylation: a key modulator of multiple receptor functions. *Molecular endocrinology (Baltimore, Md.)* **21**, 2311-2319 (2007). https://doi.org:10.1210/me.2007-0101
30 Mayr, B. & Montminy, M. Transcriptional regulation by the phosphorylation-dependent factor CREB. *Nature reviews. Molecular cell biology* **2**, 599-609 (2001). https://doi.org:10.1038/35085068
31 Zanivan, S. *et al.* Solid tumor proteome and phosphoproteome analysis by high resolution mass spectrometry. *J Proteome Res* **7**, 5314-5326 (2008). https://doi.org:10.1021/pr800599n
32 Tomanov, K. *et al.* Sumoylation and phosphorylation: hidden and overt links. *Journal of Experimental Botany* **69**, 4583-4590 (2018). https://doi.org:10.1093/jxb/ery167
33 Khan, M. *et al.* Interplay between phosphorylation and SUMOylation events determines CESTA protein fate in brassinosteroid signalling. *Nat Commun* **5**, 4687 (2014). https://doi.org:10.1038/ncomms5687
34 Wegener, A. D., Simmerman, H. K., Lindemann, J. P. & Jones, L. R. Phospholamban phosphorylation in intact ventricles. Phosphorylation of serine 16 and threonine 17 in response to beta-adrenergic stimulation. *The Journal of biological chemistry* **264**, 11468-11474 (1989).
35 Pilz, A. *et al.* Phosphorylation of the Stat1 transactivating domain is required for the response to type I interferons. *EMBO reports* **4**, 368-373 (2003). https://doi.org:10.1038/sj.embor.embor802
36 Wen, Z., Zhong, Z. & Darnell, J. E., Jr. Maximal activation of transcription by Stat1 and Stat3 requires both tyrosine and serine phosphorylation. *Cell* **82**, 241-250 (1995). https://doi.org:10.1016/0092-8674(95)90311-9
37 Kumar, A., Vaish, M. & Ratan, R. R. Transcriptional dysregulation in Huntington's disease: a failure of adaptive transcriptional homeostasis. *Drug Discov. Today* **19**, 956-962 (2014). https://doi.org:10.1016/j.drudis.2014.03.016
38 Wang, H., Xu, J., Lazarovici, P., Quirion, R. & Zheng, W. cAMP Response Element-Binding Protein (CREB): A Possible Signaling Molecule Link in the Pathophysiology of Schizophrenia. *Frontiers in molecular neuroscience* **11**, 255-255 (2018). https://doi.org:10.3389/fnmol.2018.00255
39 Seif, F. *et al.* The role of JAK-STAT signaling pathway and its regulators in the fate of T helper cells. *Cell Communication and Signaling* **15**, 23 (2017). https://doi.org:10.1186/s12964-017-0177-y
40 Decker, T. & Kovarik, P. Serine phosphorylation of STATs. *Oncogene* **19**, 2628-2637 (2000). https://doi.org:10.1038/sj.onc.1203481
41 Beurel, E., Grieco, S. F. & Jope, R. S. Glycogen synthase kinase-3 (GSK3): regulation, actions, and diseases. *Pharmacol Ther* **148**, 114-131 (2015). https://doi.org:10.1016/j.pharmthera.2014.11.016
42 Lal, H., Ahmad, F., Woodgett, J. & Force, T. The GSK-3 family as therapeutic target for myocardial diseases. *Circ Res* **116**, 138-149 (2015). https://doi.org:10.1161/circresaha.116.303613
43 Raoux, M. *et al.* Multilevel control of glucose homeostasis by adenylyl cyclase 8. *Diabetologia* **58**, 749-757 (2015). https://doi.org:10.1007/s00125-014-3445-z

816 **Figure Legends**

817 **Figure 1. TGAC8 reprograms the LV phosphorylation state. A**. PCA plot of
818 phosphoproteome in TGAC8 vs. WT LVs. **B**. Heatmap of scaled expressions of phosphorylated
819 proteins. **C**. Volcano plot of phosphoproteome. Red dots represent upregulated phosphoproteins
820 with -log10(p-value) > 1.3 and log2(fold change) ≥ 0.4; blue dots represent downregulated
821 phosphoproteins with -log10(p-value) > 1.3 and log2(fold change) ≤ -0.4; grey dots represent
822 nonsignificantly regulated phosphoproteins with -log10(p-value) ≤ 1.3 or absolute(log2(fold
823 change)) < 0.4. **D**. Top 21 canonical pathways enriched from phosphoproteome. Orange and blue
824 bars represent activated and inhibited pathways respectively. The darker the color is, the greater
825 the absolute(z-score) is, and the more significantly enriched the pathway is. **E**. Regulatory
826 pathway from upstream kinases. Three dots in the center represent the predicted upstream
827 kinases. Surrounding dots represent identified phosphoproteins differentially regulated in
828 phosphoproteome. Terms on the bottom represent canonical pathways in which the
829 phosphoproteins are involved. Meanings of colors refer to the box of prediction legend besides
830 the graph. **F**. Enriched molecular and cellular functions from the phosphoproteome. They are
831 related to three categories, including cell viability, protein quality control, and metabolism.

832

833 **Figure 1—figure supplement 1. The enriched pathway, Cardiac Hypertrophy Signaling**
834 **(Enhanced), from the phosphoproteome.** Cardiac Hypertrophy Signaling (Enhanced) is
835 visualized using IPA. Dots with purple outline are identified phosphoproteins or protein
836 complexes. Red and green fill colors indicate upregulation and downregulation respectively.

837

838 **Figure 1—figure supplement 2. The regulatory pathway under the control of a predicted**
839 **upstream kinase, PDPK1.** PDPK1 in the center is one representative of predicted upstream
840 kinases. Surrounding dots represent identified phosphoproteins differentially regulated in
841 phosphoproteome. Meanings of colors refer to the box of prediction legend besides the graph.
842 Blue glows represent that the increased phosphorylation levels inhibit the activity of
843 corresponding proteins.

844

845 **Figure 2. Characteristics of upregulated phosphopeptides. A**. Composition of phosphosites
846 that reside on the upregulated phosphopeptides. **B**. Sequence logo diagrams of upregulated
847 phosphopeptides centered on the phosphosites and flanked by 6 amino acids on the N and C
848 termini respectively using WebLogo online software. Colors of amino acids represent different
849 chemical properties. **C**. Western blots of phosphorylation of PKA substrates and their statistics
850 results: RRXS*/T*. Unpaired Student's t test with Welch's correction was used. **D**. Test the
851 amphiphilicity feature of the upregulated phosphopeptides using iceLogo online software and
852 referring to a published work by Mitaku and colleagues in 2002[13].

853

854 **Figure 3. Integrative analysis of transcriptome, proteome and phosphoproteome. A**. Circos
855 plot of gene expression at different levels from transcription, to protein, and to phosphorylation.
856 Bars in each layer of circle represent changes of significantly regulated molecules (q-value or p-
857 value < 0.05) in transcriptome, total proteome, and unnormalized phosphoproteome. Bar height,
858 color and direction represent log2(fold change). Red and upward indicate upregulation, and blue
859 and downward indicate downregulation. **B-C**. Scatter plots of correlation between

860 phosphoproteome and transcriptome (**B**) or total proteome (**C**). **D**. Comparison of canonical
861 pathway enrichments from the transcriptome, total proteome, and phosphoproteome. Enrichment
862 z-scores were calculated in IPA, and were scaled to generate heatmap in R language. **E**.
863 Integrative graph of expression of all phosphoproteins and selected types of molecules. Bar plot
864 on the bottom displays expression of all significantly changed (p-value < 0.05) phosphoproteins
865 in unnormalized phosphoproteome. Y-axis denotes log2(fold change), and x-axis denotes each
866 molecule ranked by log2(fold change). Bars were colored by -log10(p-value). Stick plots on the
867 top display kinases, phosphatases and transcription factors (TFs) selected from the bottom bar
868 plot and their changes in transcriptome (RNA), total proteome (pro), and normalized
869 phosphoproteome (norm). From top to bottom: each large block denotes the changes of certain
870 types of molecules (from kinases to phosphatases, to TFs). In each block, the three rows from top
871 to bottom indicate the changes in transcriptome, total proteome, and normalized
872 phosphoproteome. Each stick represents a molecule and color represents the change: red: (p-
873 value or q-value < 0.05) and log2FC > 0; blue: (p-value or q-value < 0.05) and log2FC < 0;
874 black: (p-value or q-value ≥ 0.05) or log2FC = 0; grey: unidentified in one of the omics. Their
875 locations are matched to those in the bottom bar plot. **F-J**. Pie plots of composition of
876 phosphoproteins in the unnormalized phosphoproteome. Regardless of p-value, numbers of four
877 types of proteins, including kinases, phosphatases, TFs and others, are displayed in **F**. After
878 filtration with cutoff p-value < 0.05, numbers of those types of proteins are displayed in **G**.
879 Extracted from G, numbers of upregulated and downregulated kinases (**H**), phosphatases (**I**) and
880 TFs (**J**) are displayed.

881

882 **Figure 4. Coordination of phosphoproteome and transcriptome. A**. GO term enrichments of
883 biological processes and molecular functions about phosphorylation and dephosphorylation from
884 transcriptome. **B-C**. Changes of kinases (**B**) and phosphatases (**C**) whose q-values are less than
885 0.05 in transcriptome. **D-E**. States of upstream kinases (**D**) and phosphatases (**E**) predicted based
886 on transcriptome. Z-scores were calculated in IPA. Positive and negative z-scores indicate
887 activated and inhibited states respectively. The larger absolute values of z-score indicate more
888 activated or inhibited states. **F**. Heatmap of predicted upstream transcription regulators (left) and
889 their changes in different omics datasets (right). Left: Fill color represent activation z-scores in
890 transcriptome and total proteome. Red and blue indicate activated and inhibited states
891 respectively. Molecules are ranked by z-scores in transcriptome. Right: Fill color represent
892 changes in transcriptome, total proteome, unnormalized phosphoproteome, and normalized
893 phosphoproteome: orange: (p-value or q-value < 0.05) and log2FC > 0; yellow: (p-value or q-
894 value ≥ 0.05) and log2FC > 0; green: (p-value or q-value < 0.05) and log2FC < 0; light blue: (p-
895 value or q-value ≥ 0.05) and log2FC < 0; grey: unidentified in one of the omics. **G**. Changes of
896 differentially regulated TFs with p-value < 0.05 in the unnormalized phosphoproteome. **H**.
897 KEGG pathway enrichments of the differentially regulated TFs. They are in four primary
898 categories: cancer, immunity, metabolism and others. **I**. Top 20 canonical pathways enriched
899 from the phosphoproteome using IPA. The darker the color is, the greater the absolute(z-score)
900 is, and the more significantly enriched the pathway is. **J**. Enriched molecular and cellular
901 functions from the phosphoproteome using IPA. They are in two primary categories: cell
902 viability and metabolism.

903

904 **Figure 5. Analysis of normalized phosphoproteome. A**. GO term enrichments of biological
905 processes and molecular functions about phosphorylation and dephosphorylation from the
906 present proteome. **B-C**. Changes of kinases (**B**) and phosphatases (**C**) whose q-values are less
907 than 0.05 in previous proteome. **D-E**. States of upstream kinases (**D**) and phosphatases (**E**)
908 predicted based on the present proteome. Z-scores were calculated in IPA. Positive and negative
909 z-scores indicate activated and inhibited states respectively. The larger absolute values of z-score
910 indicate more activated or inhibited states. **F**. Venn plot of new total proteome and unnormalized
911 phosphoproteome that were conducted concurrently in the same platform. **G**. PCA plot of
912 phosphoproteome normalized to total proteome. **H**. Heatmap of expressions of phosphoproteins
913 normalized to total proteins. **I**. Volcano plot of normalized phosphoproteome. Red dots represent
914 upregulated phosphoproteins with -log10(p-value) > 1.3 and log2(fold change) ≥ 0.4; blue dots
915 represent downregulated phosphoproteins with -log10(p-value) > 1.3 and log2(fold change) ≤ -
916 0.4; grey dots represent nonsignificantly regulated phosphoproteins with -log10(p-value) ≤ 1.3 or
917 absolute(log2(fold change)) < 0.4. **J**. Comparison of canonical pathway enrichments between
918 unnormalized and normalized phosphoproteome. Orange fill colors indicate that all comparable
919 pathways on the top are activated in both omics datasets. The darker the color is, the greater the
920 absolute(z-score) is, and the more significantly enriched the pathway is.

921

922 **Figure 6. Coordinated regulation of transcriptome, proteome and phosphoproteome on**
923 **PI3K/AKT and ERK/MAPK signaling pathways and protein synthesis and degradation. A**.
924 Canonical pathway enrichment of phosphoproteome only with cutoff p-value < 0.05. The darker
925 the color is, the greater the absolute(z-score) is, and the more significantly enriched the pathway
926 is. **B**. Comparison of PI3K/AKT signaling and protein ubiquitination pathways enriched from

927 transcriptome (red outline), proteome (blue outline) and phosphoproteome (green outline). **C-D**.
928 Western blots of two phosphorylation sites on pan-AKT protein for verification of
929 phosphorylation and activation of PI3K/AKT signaling pathway in TGAC8 vs. WT. **E**. Western
930 blot of ubiquitination in TGAC8 vs. WT. **F**. Pathway graph of PI3K/AKT signaling marked with
931 changes in transcriptome (left box), proteome (middle box) and phosphoproteome (right box).
932 Fill colors indicate changes: red and green indicate upregulation and downregulation
933 respectively; grey indicates nonsignificant regulation. **G**. Phosphopeptide number of substrates
934 of PI3K. Y-axis represents protein substates of PI3K; x-axis represents number of
935 phosphopeptides. Red and blue bars indicate upregulated (p-value < 0.05 and log2(fold
936 change) > 0) and downregulated (p-value < 0.05 and log2(fold change) < 0) phosphopeptides
937 respectively. Two-tailed unpaired Student's t test with Welch's correction was conducted and p-
938 values were shown in plots.

939

940 **Figure 6—figure supplement 1. Cross verification of activated PI3K/AKT and ERK/MAPK**
941 **signaling pathways and enhanced protein synthesis and degradation from our previous**
942 **study. A.** Western blots of one phosphorylation site on isoform 2 of AKT protein for verification
943 of phosphorylation and activation of PI3K/AKT signaling pathway in TGAC8 vs. WT. **B-C.**
944 Western blot verification of phosphorylation and activation of ERK/MAPK signaling pathway in
945 TGAC8 vs. WT. **D.** Confirmation of enhanced protein synthesis in TGAC8 vs. WT. **E.** The
946 enhanced proteasome activity in TGAC8 vs. WT. **F-G.** The soluble misfolded proteins were
947 increased in TGAC8 LV (**F**) whereas the insoluble protein aggregates did not accumulate within
948 the TGAC8 vs. WT (**G**). Two-tailed unpaired Student's t test with Welch's correction was

949 performed. P-values: * < 0.05, ** < 0.01, *** < 0.001, **** < 0.0001. These data were adapted
950 from our recently published study in TGAC8 and WT mice[5].

951

952 **Figure 7. Analyses of proteins changed discordantly in proteome and phosphoproteome. A**.
953 Venn diagram of significantly regulated proteins in total proteome and significantly regulated
954 phosphoproteins in unnormalized phosphoproteome that were conducted concurrently in the
955 same platform. **B-D**. Functional analyses of proteins whose expressions are changed discordantly
956 at total protein and phosphorylation levels. Mitochondria and others are enriched in cellular
957 component analysis (**B**). Functions related to metabolism, mitochondria and others are enriched
958 in Reactome pathway (**C**) and biological process analyses (**D**).

959

960 **Figure 8. Deduced schematic of coordination of phosphoproteome with transcriptome and**
961 **proteome in TGAC8 mouse LV.** Based on our results, we deduced a mechanism of
962 reprogramed phosphoproteome in TGAC8 mouse LV: First, TGAC8 mouse induces a PKA
963 dependent phosphorylation via AC8-cAMP-PKA axis. Many cytoplasmic proteins including TFs
964 are thus phosphorylated and then transported into the nuclear where TFs recognize and bind to
965 the promotors to activate the transcription of more regulatory factors, including kinases,
966 phosphatases, and TFs. The activation states of these factors are changed upon phosphorylated in
967 cytosol, thereby activating additional kinases-controlled phosphorylation cascades and
968 reprogramming the cardiac phosphoproteome comprehensively. Left column: AC8-cAMP-PKA
969 signaling; middle column: phosphorylation (phosphoproteome); lower right: transcription
970 (transcriptome); upper right: translation (proteome).

971

972 **Appendix 1. Reprogrammed concentric performance and protection circuitry in response**
973 **to the constitutive challenge of marked cardiac-specific overexpression of adenylyl cyclase**
974 **type 8.** Based on the present phosphoproteome, we optimized our previously deduced
975 mechanism graph and labeled findings from the phosphoproteome using red stars. TGAC8
976 mouse induces a chronic cardiac exercise on heart, manifested as increased heart rate and
977 contractility accompanied with increased energy demand and cardiac biomass. Multiple
978 signaling pathways, related to nutrient sensing, energy production, cardiac cellular stress, cardiac
979 stress response, growth factor signaling, and cell proliferation, are potential downstream
980 mediating the effect of the activated AC8-cAMP-PKA-Ca^{2+} signaling in mouse LV. The altered
981 cardiac functions were also observed associated with protein phosphorylation in our previous
982 study and labeled in blue star here.

983

984 **Figures**

985 **Figure 1. TGAC8 reprograms the LV phosphorylation state.**

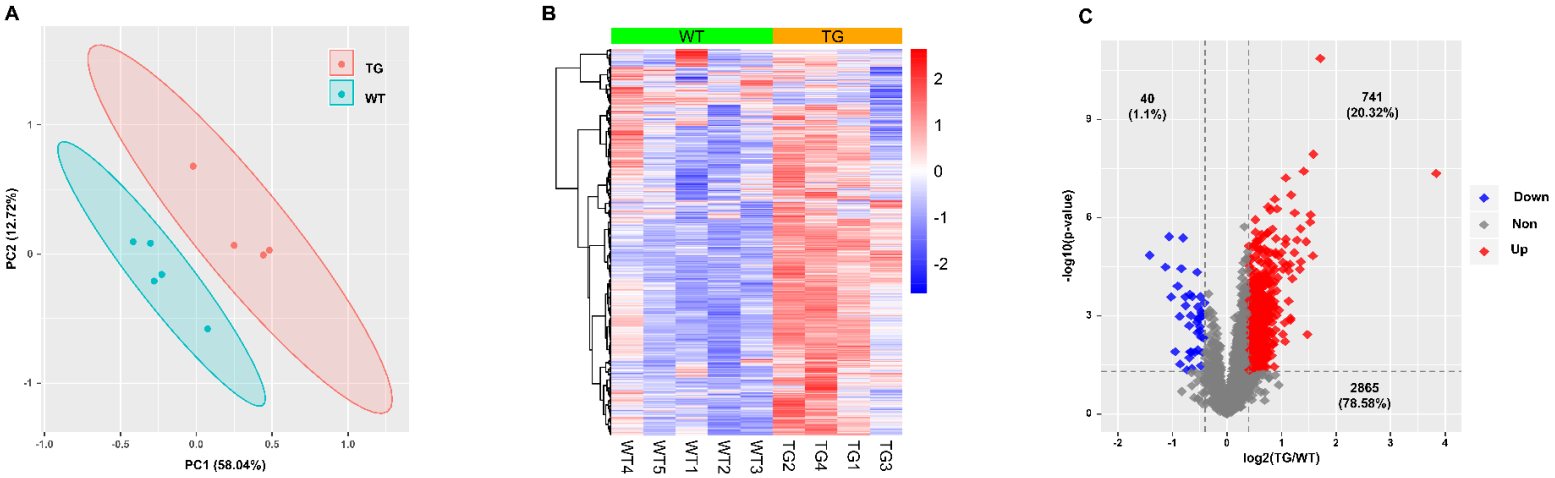
A
TG
WT
PC2 (12.72%)
PC1 (58.04%)
B
WT
TG
WT4
WT5
WT1
WT2
WT3
TG2
TG4
TG1
TG3
C
40
(1.1%)
741
(20.32%)
2865
(78.58%)
-log10(p-value)
log2(TG/WT)
Down
Non
Up

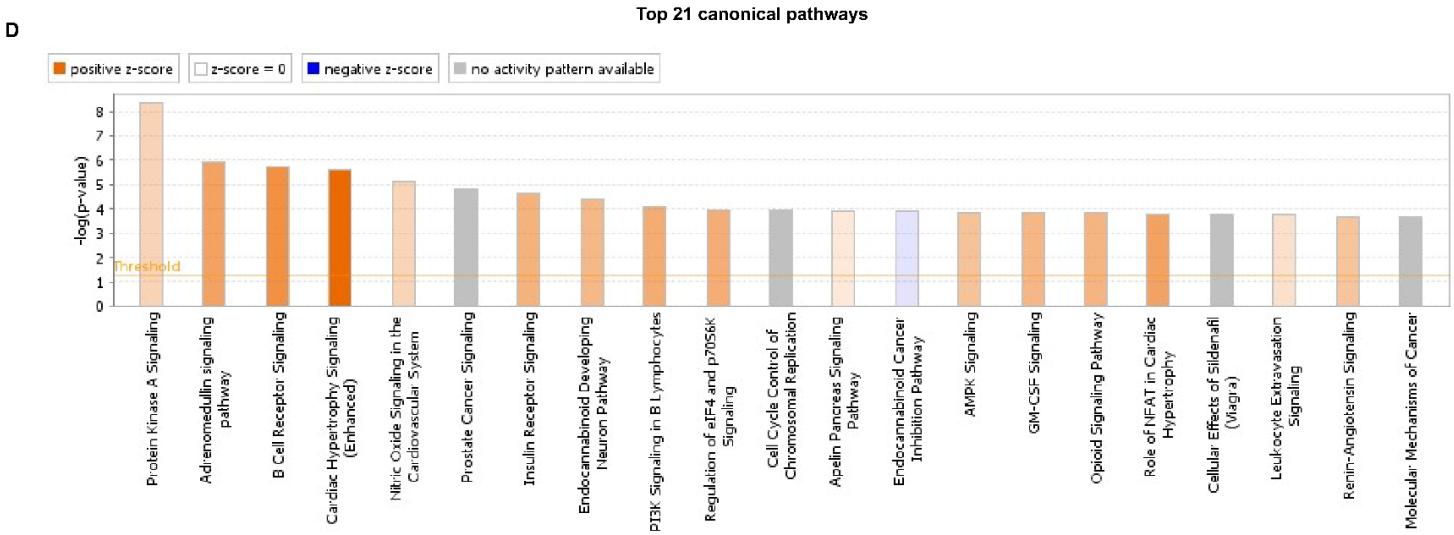
D
Top 21 canonical pathways
positive z-score
z-score = 0
negative z-score
no activity pattern available
-log(p-value)
Threshold
Protein Kinase A Signaling
Adrenomedullin signaling pathway
B Cell Receptor Signaling
Cardiac Hypertrophy Signaling (Enhanced)
Nitric Oxide Signaling in the Cardiovascular System
Prostate Cancer Signaling
Insulin Receptor Signaling
Endocannabinoid Developing Neuron Pathway
PI3K Signaling in B Lymphocytes
Regulation of eIF4 and p70S6K Signaling
Cell Cycle Control of Chromosomal Replication
Apelin Pancreas Signaling Pathway
Endocannabinoid Cancer Inhibition Pathway
AMPK Signaling
GM-CSF Signaling
Opioid Signaling Pathway
Role of NFAT in Cardiac Hypertrophy
Cellular Effects of Sildenafil (Magra)
Leukocyte Extravasation Signaling
Renin-Angiotensin Signaling
Molecular Mechanisms of Cancer

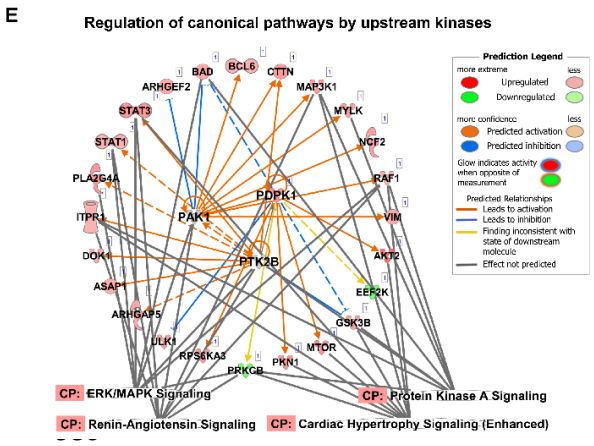
E
Regulation of canonical pathways by upstream kinases
Prediction Legend
Upregulated
Downregulated
Predicted activation
Predicted inhibition
Effect not predicted
BAD
BCL6
CTTN
ARHGEF2
MAP3K1
STAT3
MYLK
STAT1
NCF2
PLA2G4A
RAF1
PDPK1
ITPR1
PAK1
VIM
DOK4
PTK2B
AKT2
ASAP1
EEF2K
ARHGAP5
GSK3B
ULK1
MTOR
RPS6KA3
PKN1
PRKCB
CP: ERK/MAPK Signaling
CP: Protein Kinase A Signaling
CP: Renin-Angiotensin Signaling
CP: Cardiac Hypertrophy Signaling (Enhanced)

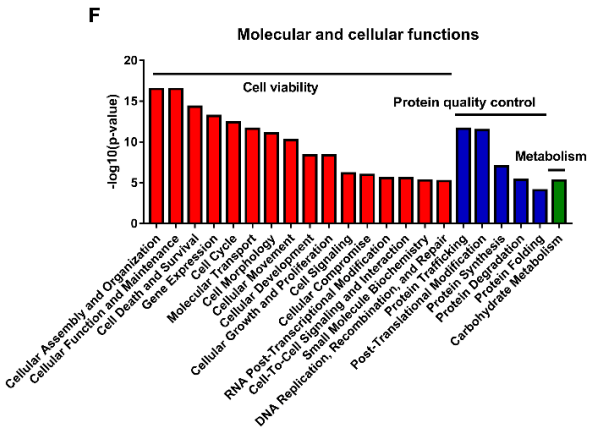
F
Molecular and cellular functions
-log10(p-value)
Cell viability
Protein quality control
Metabolism
Cellular Assembly and Organization
Cellular Function and Maintenance
Cell Death and Survival
Gene Expression
Cell Cycle
Molecular Transport
Cell Morphology
Cellular Movement
Cellular Development
Cellular Growth and Proliferation
Cell Signaling
Cellular Compromise
RNA Post-Transcriptional Modification
Small Molecule Biochemistry
DNA Replication, Recombination, and Repair
Protein Trafficking
Post-Translational Modification
Protein Synthesis
Protein Degradation
Protein Folding
Carbohydrate Metabolism

987 **Supplementary Figure 1. The enriched pathway, Cardiac Hypertrophy Signaling (Enhanced), from**

988 **the phosphoproteome.**

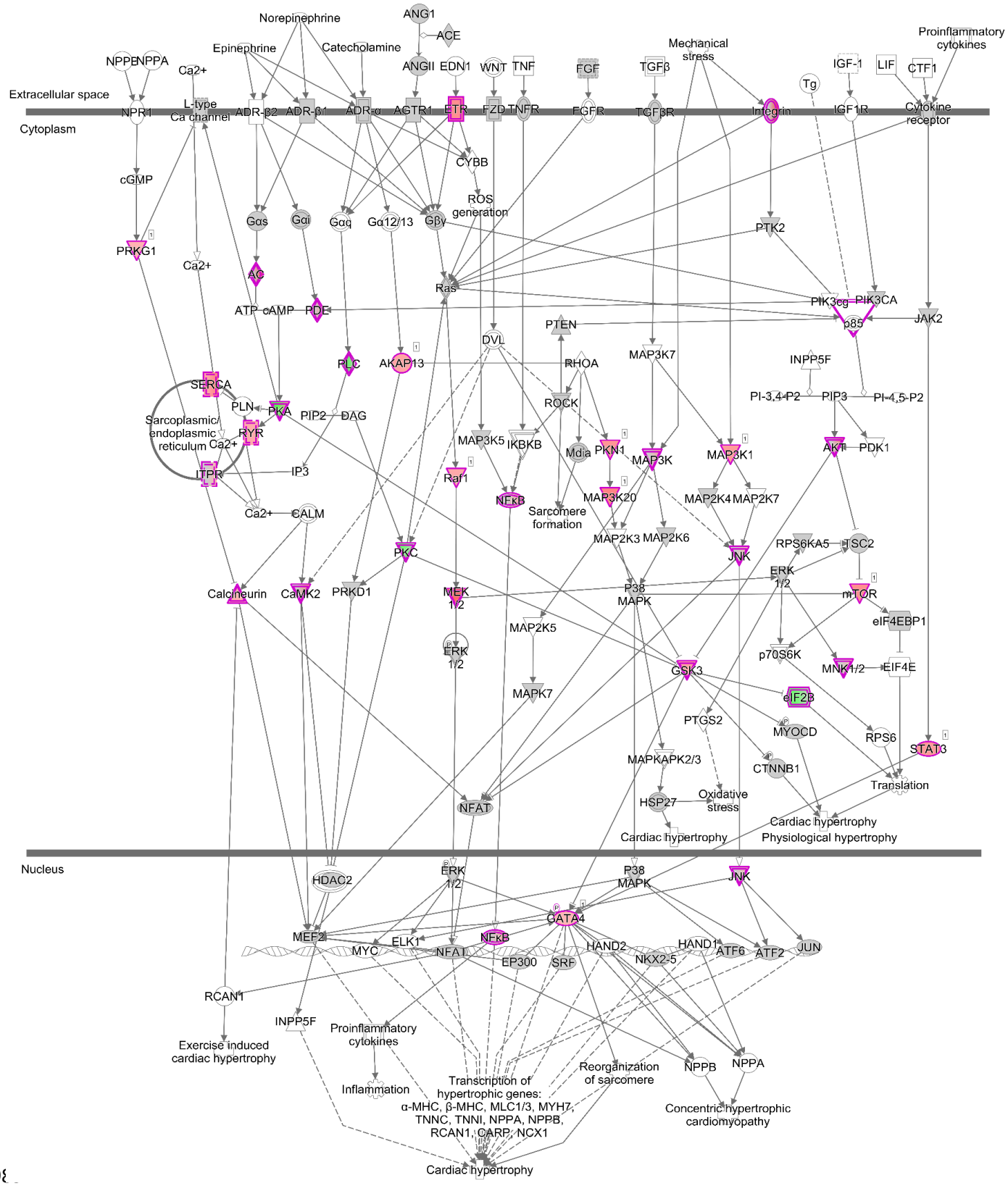
Extracellular space
Cytoplasm
Nucleus
Norepinephrine
Epinephrine
Catecholamine
ANG1
ACE
ANGII
EDN1
WNT
TNF
FGF
TGFβ
Mechanical stress
Proinflammatory cytokines
IGF-1
LIF
CTF1
Tg
NPPB
NPPA
Ca2+
L-type Ca channel
NPR1
ADR-β2
ADR-β1
ADR-α
AGTR1
ETR
FZD
TNFR
FGFR
TGFβR
Integrin
IGF1R
Cytokine receptor
CYBB
ROS generation
cGMP
PRKG1
Gαs
Gαi
Gαq
Gα12/13
Gβγ
PTK2
AC
Ras
ATP
cAMP
PDE
PIK3cg
PIK3CA
p85
JAK2
PTEN
DVL
PLC
AKAP13
RHOA
MAP3K7
INPP5F
SERCA
PLN
PKA
PIP2
DAG
ROCK
PI-3,4-P2
PIP3
PI-4,5-P2
Sarcoplasmic/ endoplasmic reticulum
RYR
Ca2+
ITPR
IP3
MAP3K5
IKBKB
Mdia
PKN1
MAP3K
MAP3K1
AKT
PDK1
Raf1
NFκB
MAP3K20
MAP2K4
MAP2K7
Sarcomere formation
Ca2+
CALM
MAP2K3
MAP2K6
JNK
RPS6KA5
TSC2
PKC
ERK 1/2
Calcineurin
CaMK2
PRKD1
MEK 1/2
P38 MAPK
mTOR
eIF4EBP1
MAP2K5
ERK 1/2
p70S6K
MNK1/2
EIF4E
GSK3
MAPK7
eIF2B
PTGS2
MYOCD
RPS6
STAT3
MAPKAPK2/3
CTNNB1
Translation
HSP27
Oxidative stress
NFAT
Cardiac hypertrophy
Cardiac hypertrophy
Physiological hypertrophy
HDAC2
ERK 1/2
P38 MAPK
JNK
GATA4
MEF2
MYC
ELK1
NFAT
NFκB
EP300
SRF
HAND2
NKX2-5
HAND1
ATF6
ATF2
JUN
RCAN1
INPP5F
Proinflammatory cytokines
Exercise induced cardiac hypertrophy
Inflammation
Transcription of hypertrophic genes: α-MHC, β-MHC, MLC1/3, MYH7, TNNC, TNNI, NPPA, NPPB, RCAN1, CARP, NCX1
Reorganization of sarcomere
NPPB
NPPA
Concentric hypertrophic cardiomyopathy
Cardiac hypertrophy

98

990 **Supplementary Figure 2. The regulatory pathway under the control of a predicted**

991 **upstream kinase, PDPK1.**

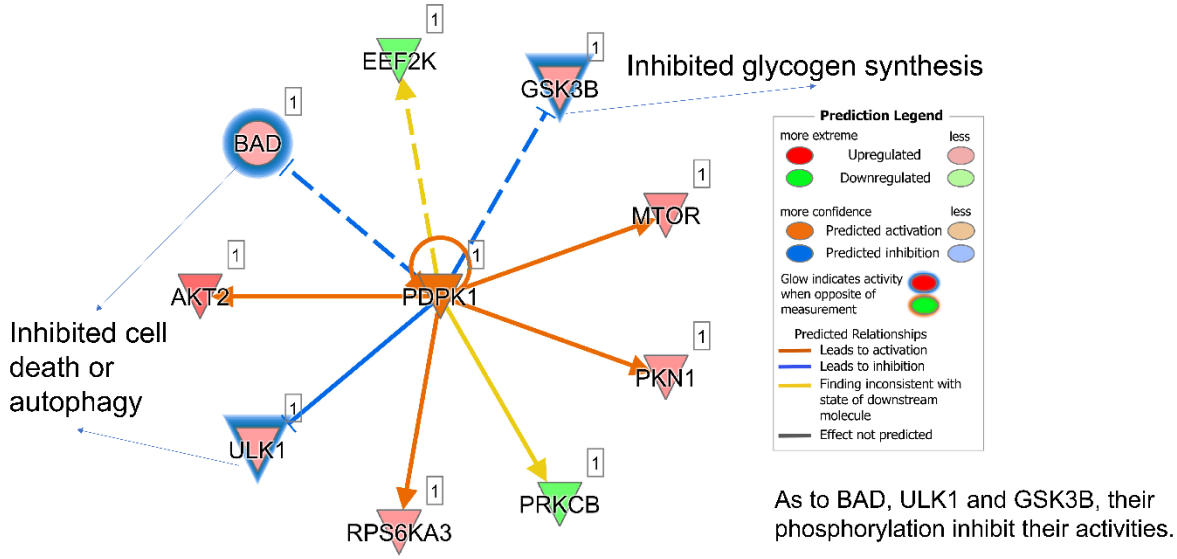

Symbol	Entrez Gene Name	UniProt	Log Ratio	p-value	Location	Family
AKT2	AKT serine/threonine kinase 2	Q60823	0.840825	0.007813	Cytoplasm	kinase
BAD	BCL2 associated agonist of cell death	Q61337	0.476462	7.81E-06	Cytoplasm	other
EEF2K	eukaryotic elongation factor 2 kinase	O08796	-0.42591	0.004744	Cytoplasm	kinase
GSK3B	glycogen synthase kinase 3 beta	Q9WV60	0.556065	0.002741	Nucleus	kinase
MTOR	mechanistic target of rapamycin kinase	Q9JLN9	0.640641	0.000144	Nucleus	kinase
PDPK1	3-phosphoinositide dependent protein kinase 1	Q9Z2A0	0.651174	0.02451	Cytoplasm	kinase
PKN1	protein kinase N1	P70268-2	0.600171	0.007485	Cytoplasm	kinase
PRKCB	protein kinase C beta	P68404-2	-0.44609	0.001011	Cytoplasm	kinase
RPS6KA3	ribosomal protein S6 kinase A3	P18654	0.580733	0.005794	Cytoplasm	kinase
ULK1	unc-51 like autophagy activating kinase 1	O70405	0.549454	0.015177	Cytoplasm	kinase

992

993

994

995

996

997

998

999 **Figure 2. Characteristics of upregulated phosphopeptides.**

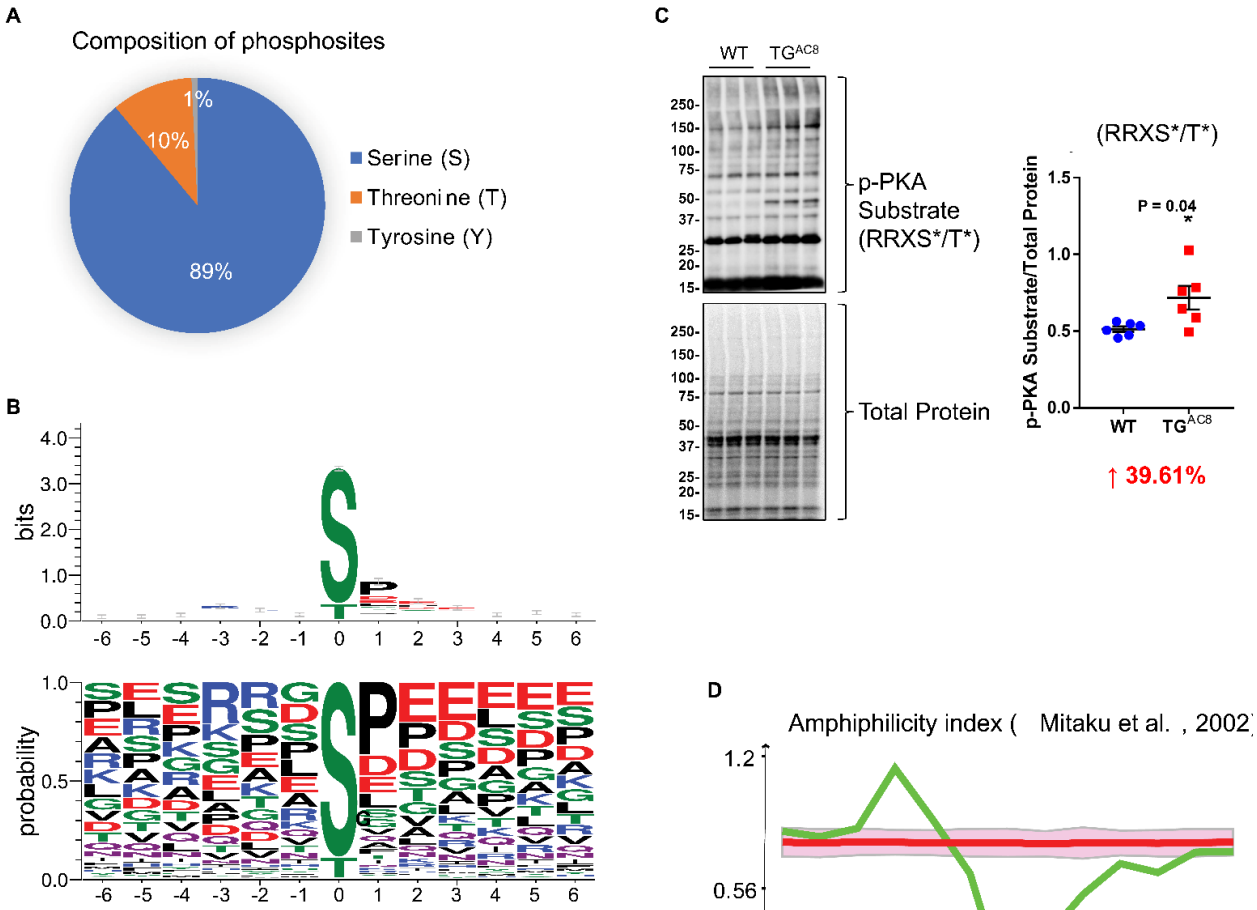

Polar	G,S,T,Y,C	green
Neutral	Q,N	purple
Basic	K,R,H	black
Acidic	D,E	red
Hydrophobic	A,V,L,I,P,W,F,M	black

1000

1001

1002

1003

1004

1005

1006 **Figure 3. Integrative analysis of transcriptome, proteome and phosphoproteome.**

1007

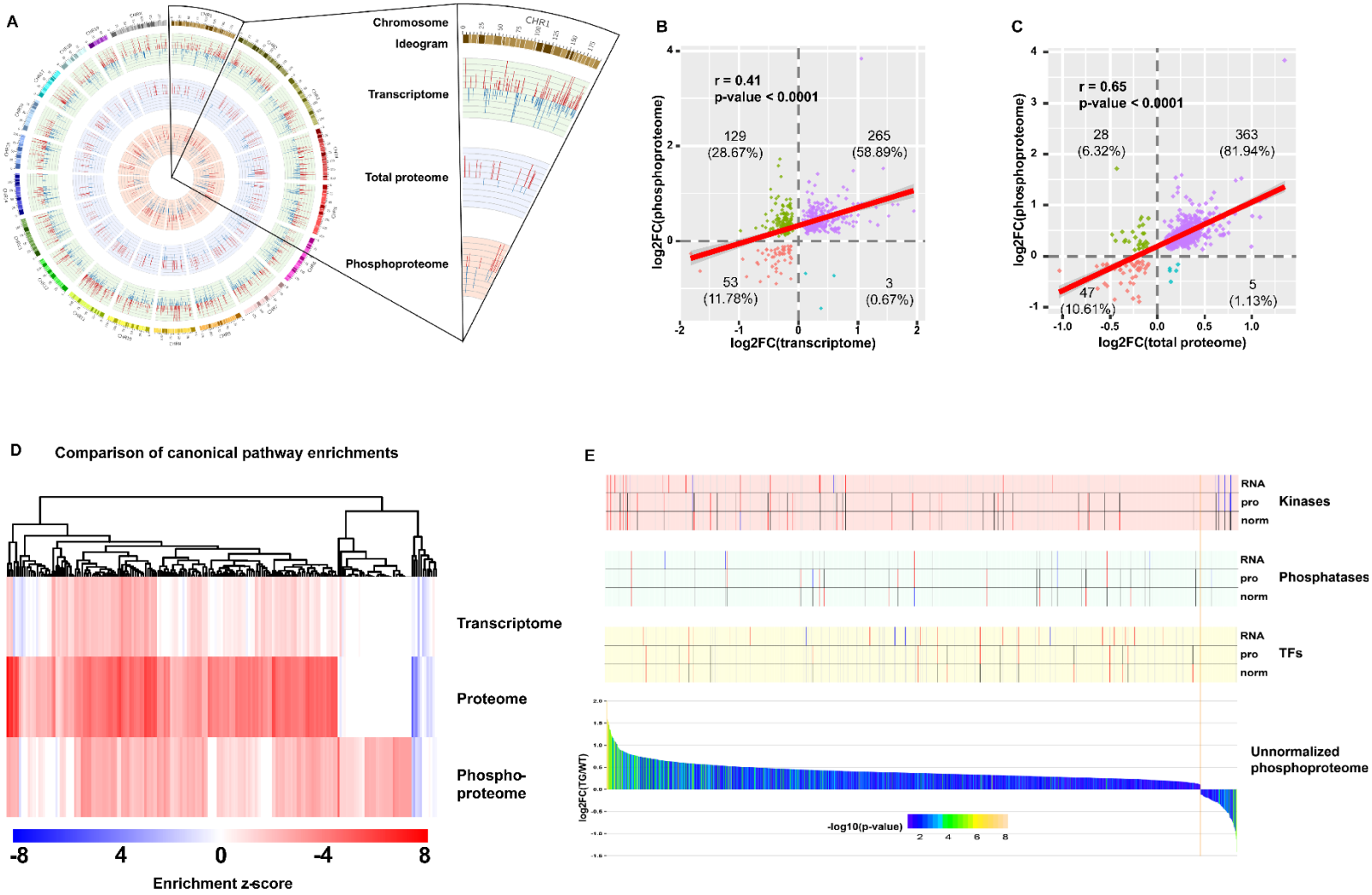

1009

1010

1011 **Figure 4. Coordination of phosphoproteome and transcriptome.**

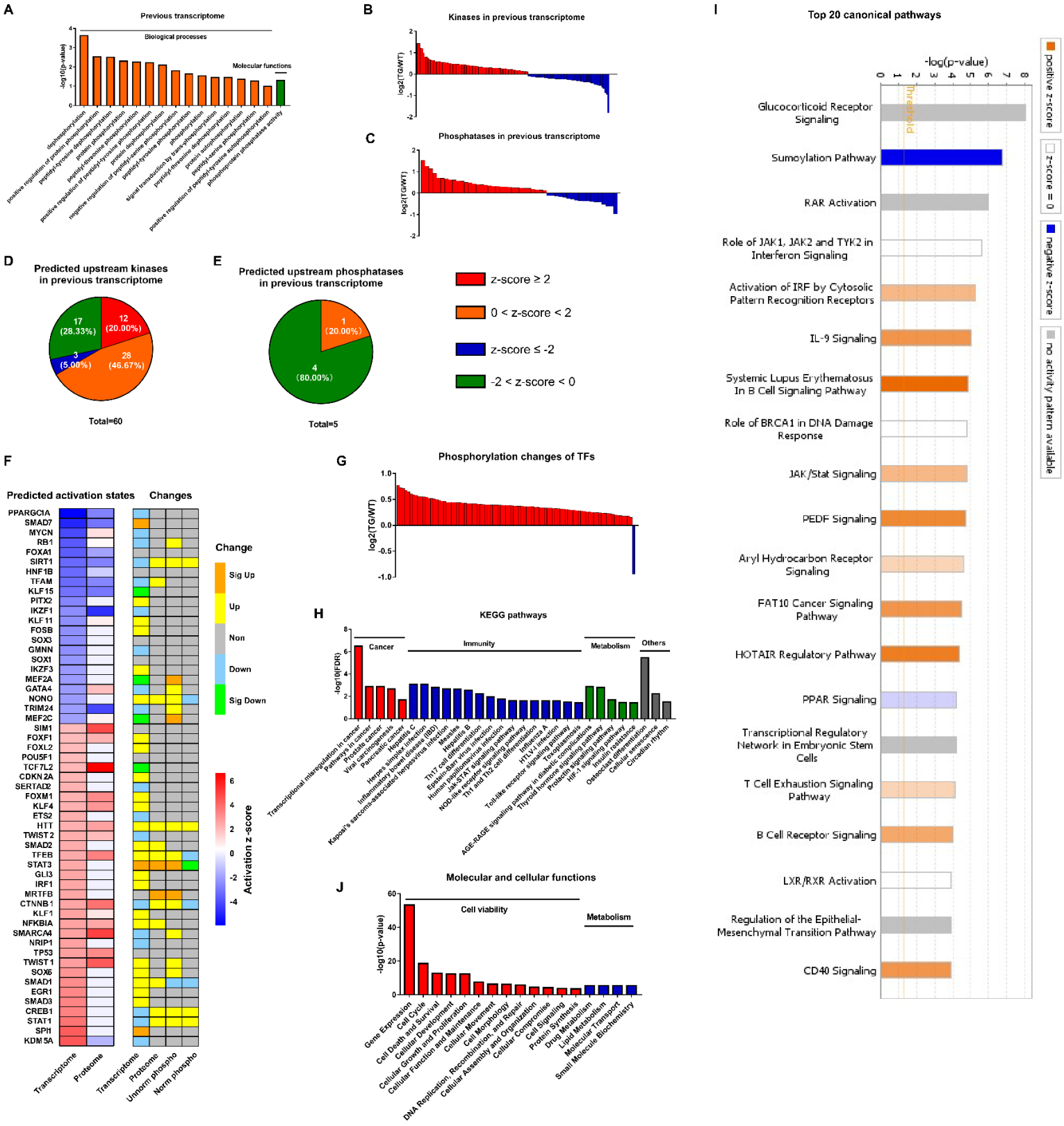

1013 **Figure 5. Analysis of normalized phosphoproteome.**

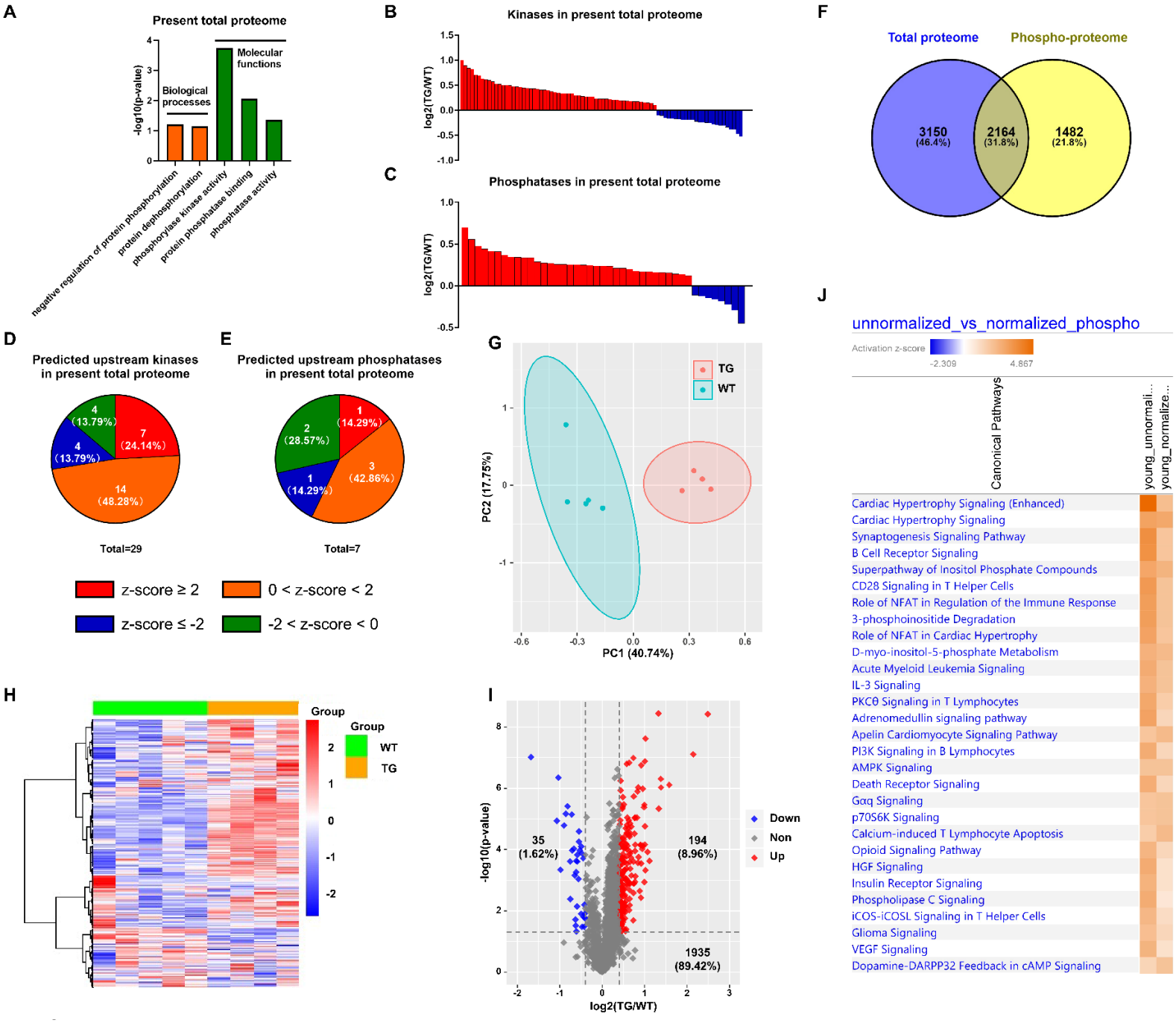

1015

1016

Figure 6. Coordinated regulation of transcriptome, proteome and phosphoproteome on PI3K/AKT and ERK/MAPK signaling pathways and protein synthesis and degradation.

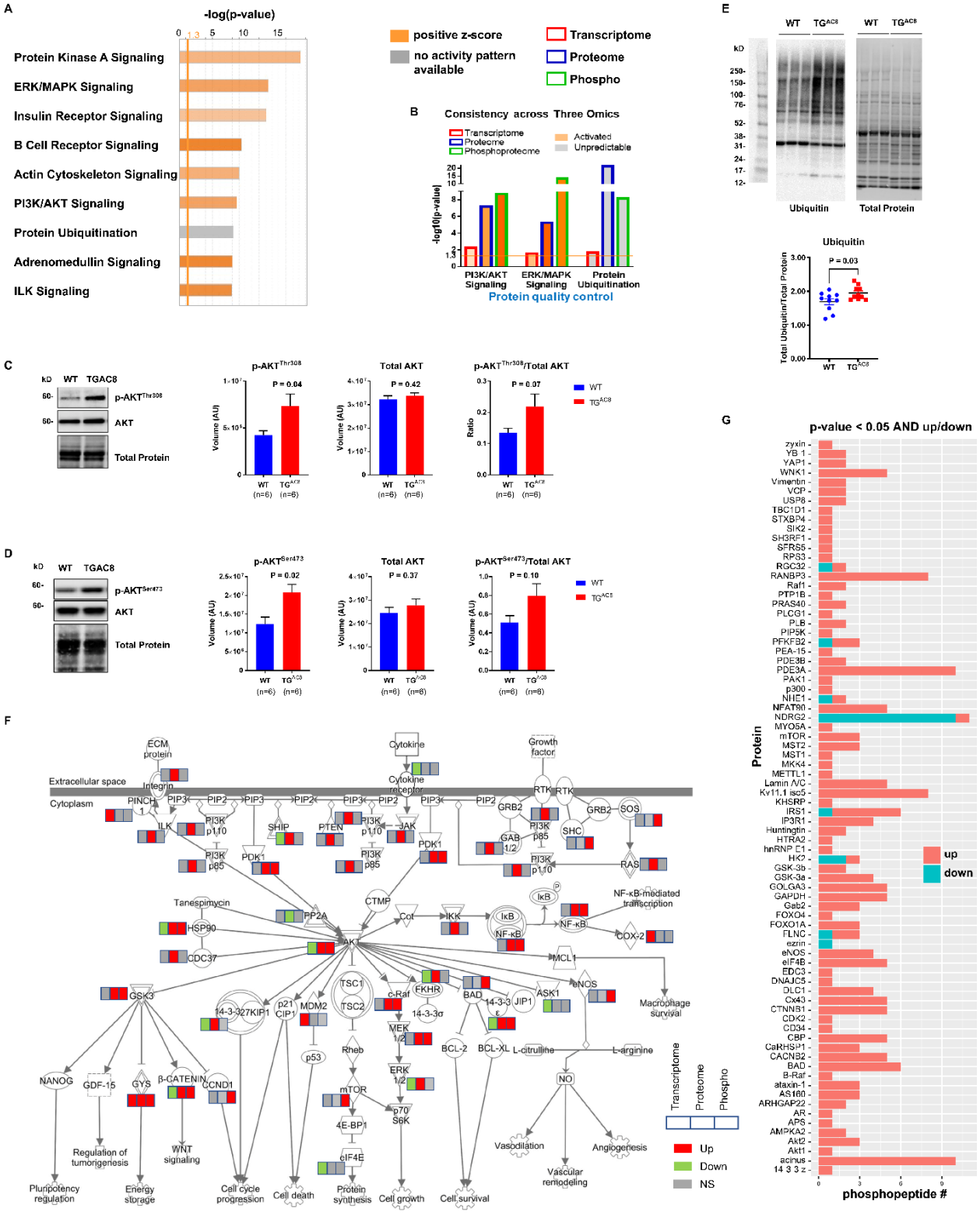

1020 **Figure 6—figure supplement 1. Cross verification of activated PI3K/AKT and ERK/MAPK**

1021 **signaling pathways and enhanced protein synthesis and degradation from our previous**

1022 **study.**

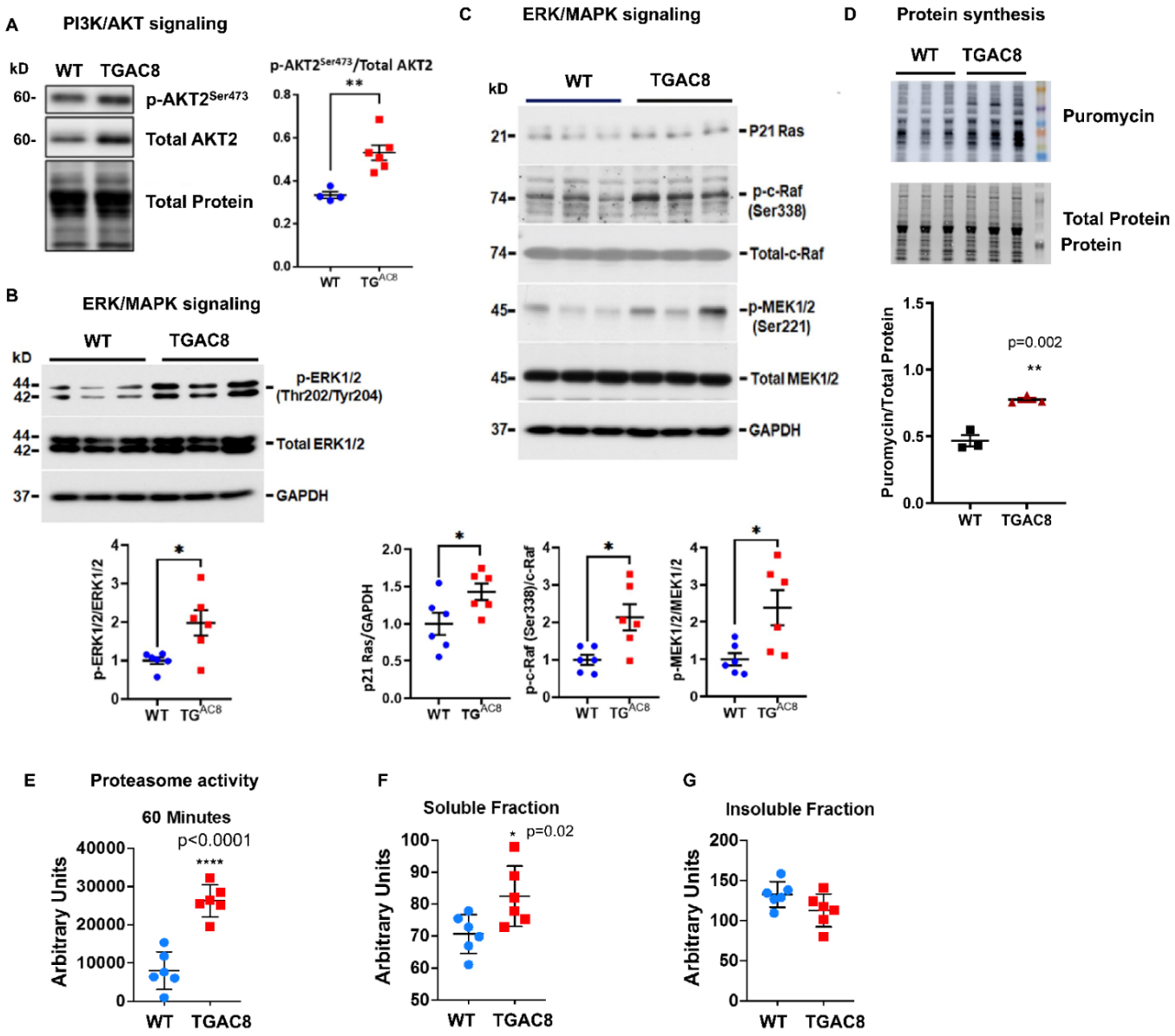

1023

1024

1025

1026 **Figure 7. Analyses of proteins changed discordantly in proteome and phosphoproteome.**

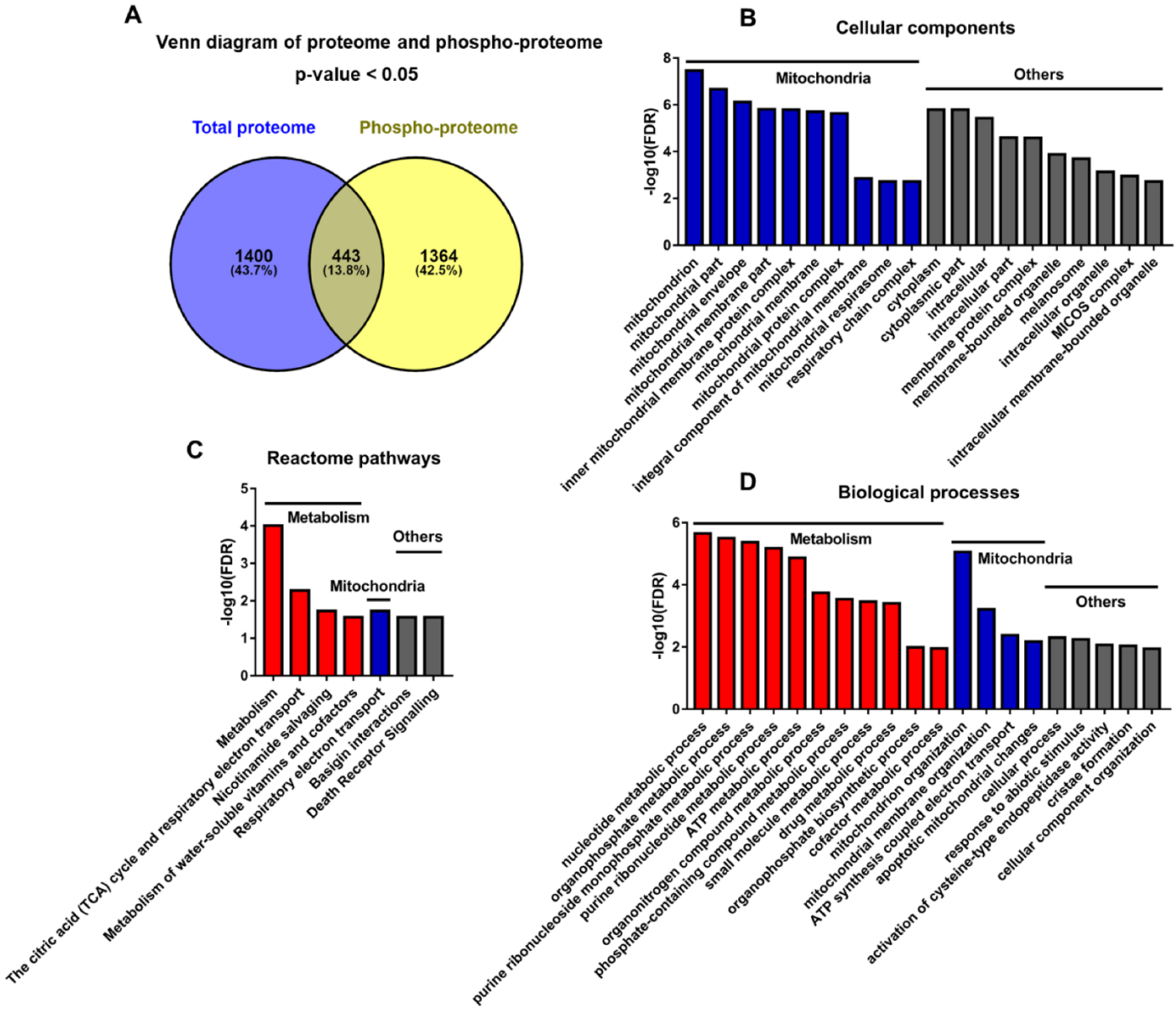

1028

1029

1030

1031

1032 **Figure 8. Deduced schematic of coordination of phosphoproteome with transcriptome and**

1033 **proteome in TGAC8 mouse LV.**

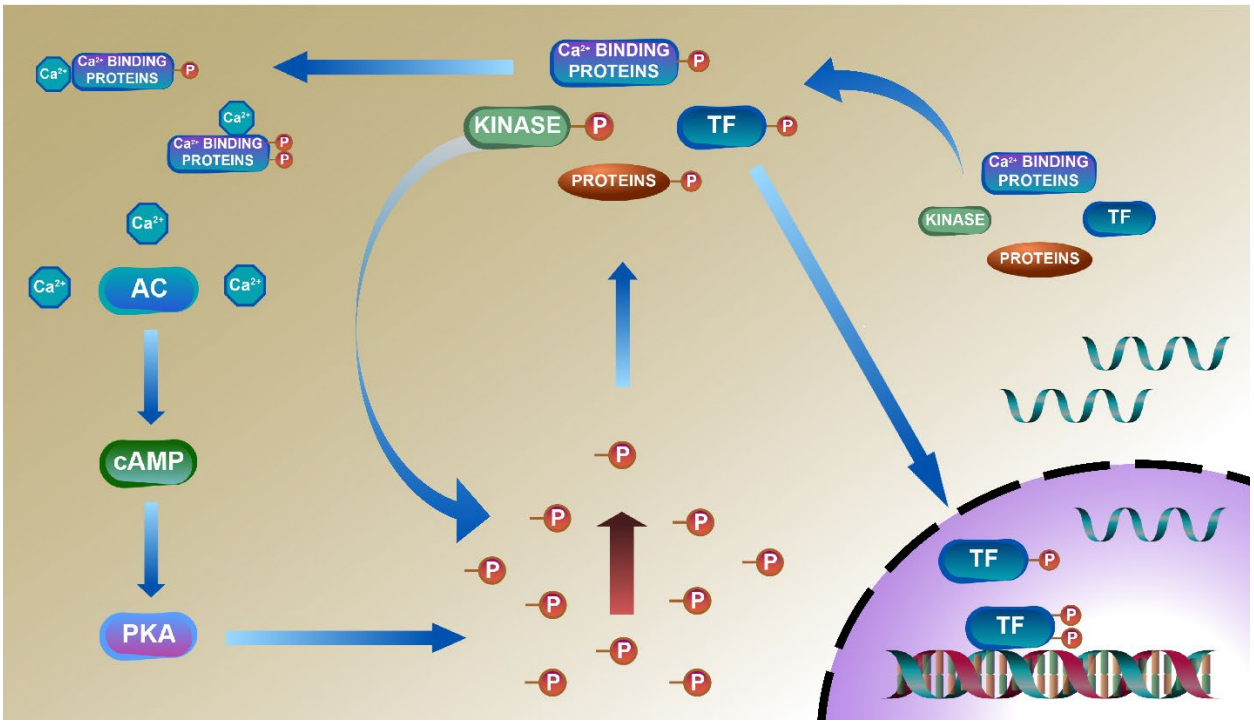

1034

1035

1036

1037

1038

1039

1040

1041

1042 **Appendix 1. A comprehensive circuitry of TGAC8 mouse heart concluded from this**

1043 **phosphoproteome combine with previous transcriptome and proteome.**

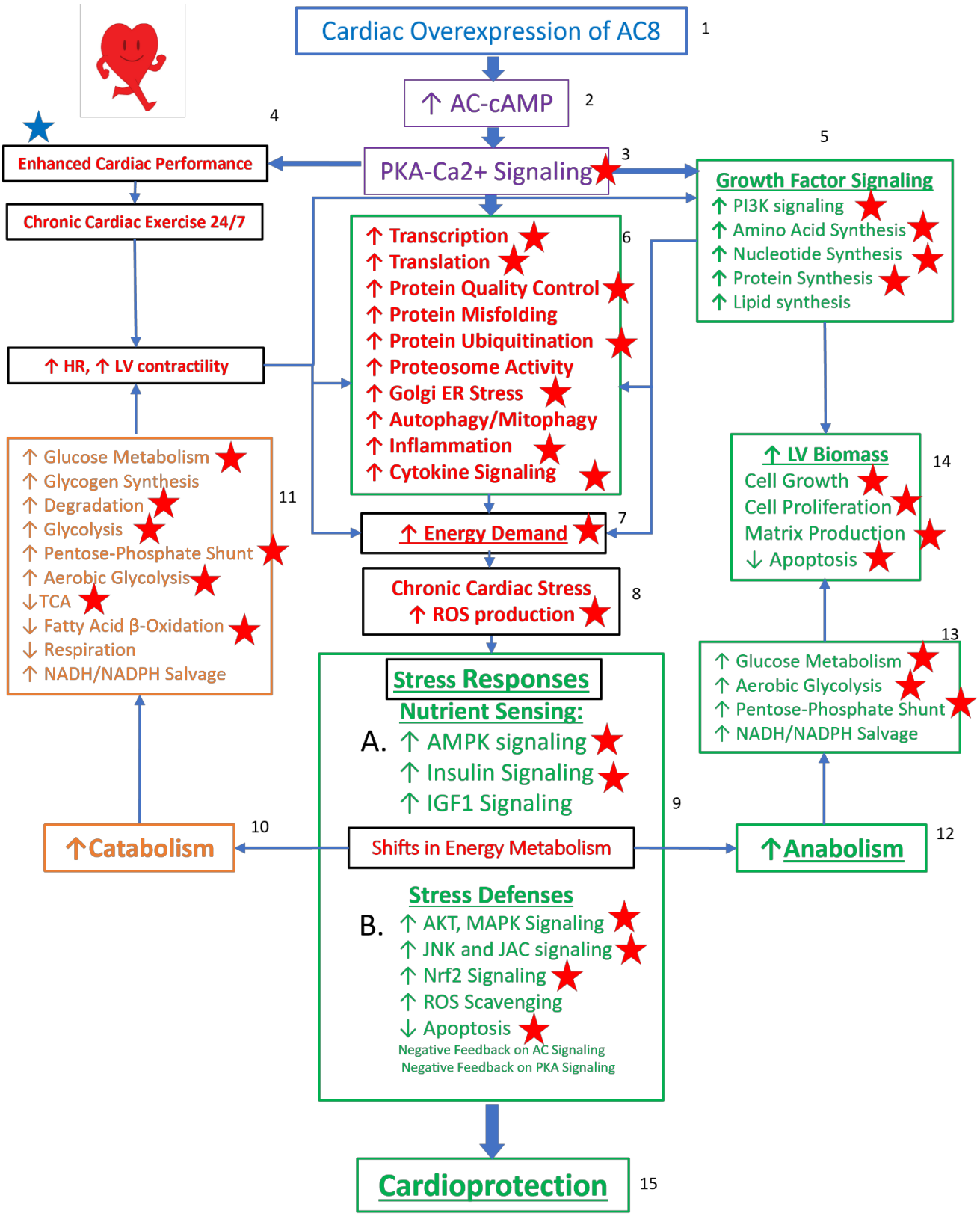
Cardiac Overexpression of AC8
1
↑ AC-cAMP
2
PKA-Ca2+ Signaling
3
4
Enhanced Cardiac Performance
Chronic Cardiac Exercise 24/7
↑ HR, ↑ LV contractility
5
Growth Factor Signaling
↑ PI3K signaling
↑ Amino Acid Synthesis
↑ Nucleotide Synthesis
↑ Protein Synthesis
↑ Lipid synthesis
6
↑ Transcription
↑ Translation
↑ Protein Quality Control
↑ Protein Misfolding
↑ Protein Ubiquitination
↑ Proteosome Activity
↑ Golgi ER Stress
↑ Autophagy/Mitophagy
↑ Inflammation
↑ Cytokine Signaling
7
↑ Energy Demand
8
Chronic Cardiac Stress
↑ ROS production
11
↑ Glucose Metabolism
↑ Glycogen Synthesis
↑ Degradation
↑ Glycolysis
↑ Pentose-Phosphate Shunt
↑ Aerobic Glycolysis
↓TCA
↓ Fatty Acid β-Oxidation
↓ Respiration
↑ NADH/NADPH Salvage
14
↑ LV Biomass
Cell Growth
Cell Proliferation
Matrix Production
↓ Apoptosis
13
↑ Glucose Metabolism
↑ Aerobic Glycolysis
↑ Pentose-Phosphate Shunt
↑ NADH/NADPH Salvage
Stress Responses
Nutrient Sensing:
A.
↑ AMPK signaling
↑ Insulin Signaling
↑ IGF1 Signaling
9
10
↑Catabolism
Shifts in Energy Metabolism
12
↑Anabolism
Stress Defenses
B.
↑ AKT, MAPK Signaling
↑ JNK and JAC signaling
↑ Nrf2 Signaling
↑ ROS Scavenging
↓ Apoptosis
Negative Feedback on AC Signaling
Negative Feedback on PKA Signaling
Cardioprotection
15

1044